Low-lying collective excitations of nuclei as a semiclassical response

A. M. Gzhebinsky, A. G. Magner,* and S. N. Fedotkin
Institute for Nuclear Research, Kyiv 03680, Ukraine
(Received 22 August 2007; revised manuscript received 16 October 2007; published 17 December 2007)

For the low-lying multipole collective excitations in nuclei, the transport coefficients of the response function theory, such as the inertia and the friction, are derived within the periodic orbit theory in the lowest orders of semiclassical expansion corresponding to the extended Thomas-Fermi approach with the surface and the curvature corrections. The collective vibrations near the spherical shape are described in the mean-field approximation through the spherical edgelike potential by using a statistical averaging of the transport coefficients. It is shown that the inertia of the collective motion is significantly larger than that of irrotational hydrodynamical flow. For large enough particle numbers in the nucleus, the mean energies of quadrupole and octupole low-lying collective vibrations, their sum rule contributions, and reduced transition probabilities are in reasonable agreement with experimental data.

DOI: 10.1103/PhysRevC.76.064315 PACS number(s): 21.60.Ev, 24.10.Nz, 23.20.−g, 21.10.Pc

I. INTRODUCTION

The collective dynamics of complex nuclei at low excitation energies, such as the vibration modes, can be described within several theoretical approaches [1–3]. One of the most powerful tools for its description is based on the response function theory [1,4], also within the semiclassical approaches [5–7]. The collective variables are introduced explicitly as deformation parameters of a mean single-particle field. In Ref. [4], the nuclear collective excitations are parametrized in terms of the transport coefficients such as the stiffness, inertia, and friction parameters through the adequate collective response functions.

The quantum formulation of a rather complicated many-body dynamical problem can be significantly simplified [8,9] by using the Strutinsky shell correction method (SCM) [10–12]. The SCM is based on the concept of the existence of the quasiparticle spectrum near the Fermi surface by the Migdal theory of finite fermion systems with a strong interaction of the particles [2]. Within this concept, for instance, the shell component of free energy can be considered perturbatively as a quasiparticle correction to the total nuclear free energy on the basis of the statistically averaged (macroscopic) background described phenomenologically through the liquid drop model or the extended Thomas-Fermi (ETF) approach [12].

Within the periodic orbit theory (POT) [12–15], so successful for its semiclassical description of the nuclear shell structure [12,14–16] and extended to the response functions of collective dynamics [17], it would be worth applying first the ideas of the SCM averaging and POT at a few lowest orders in $\hbar$, as in the ETF approach, for calculations of the smooth transport coefficients at low excitation energies. The semiclassical derivations of the famous wall formula for the average friction, owing to collisions of particles of the perfect Fermi gas with a slowly moving surface of the mean-field edgelike potential, were suggested in Refs. [18–20], see also the derivations of the wall formula in Refs. [6,21,22]. The explicit analytical expressions of a smooth inertia for the low-lying nuclear collective excitations within the semiclassical Gutzwiller path-integral approach to the POT [13,15] at leading orders in $\hbar$, with the main focus on the consistency condition [1,4,23] between the variations of potential and particle density, were studied in Ref. [24]. Many-body collective dynamics near the edge of the nucleus was described in terms of the effective nuclear surface (ENS, the points of the maximal particle-density gradient) by employing a macroscopic averaging in phase-space variables [8,25,26]. The ENS approximation [25,26] as an expansion in the leptodermic parameter (the ratio of the diffuseness parameter to a size of nucleus with A nucleons, $\sim A^{-1/3}$) was used for derivations of the dynamical equations with macroscopic boundary conditions of the liquid and Fermi-liquid drop models [25,27–30].

The main scope of this paper is the semiclassical calculation of the response function at small frequencies in terms of the averaged transport coefficients by using a more traditional way in order to study also the reduced transition probabilities and contributions to the energy-weighted sum rule (EWSR) of the low-lying collective states [1]. The key point of these derivations is to show analytically a significant enhancement of the ETF inertia with respect to that of the hydrodynamical (irrotational-flow liquid drop) model. Following Ref. [4], we begin with a general response function formalism in Sec. II. The semiclassical transport coefficients averaged macroscopically in phase-space variables (in particular, over many single-particle states near the Fermi surface) are obtained in the case of a spherical edgelike potential for the mean field at equilibrium in Sec. III. The coupling constants and the consistent collective transport coefficients for such potentials while accounting for important surface and curvature corrections of the next order in $\hbar$ are obtained in suitable variables in Sec. IV. The statistically mean vibration energies of the low-lying collective states and their EWSR contributions are derived in terms of the analytical functions of nuclear particle number in Sec. V. The reduced probabilities for the direct radiation decay of γ quanta and the corresponding lifetimes of nuclei are discussed in Sec. VI. These analytical results for the low-lying quadrupole and octupole collective modes are compared with experimental data [31–33] in Sec. VII. They are summarized

*magner@kinr.kiev.ua

in the conclusion section. Some details of the derivations are presented in Appendices A–D.

II. RESPONSE THEORY AND TRANSPORT COEFFICIENTS

Many-body collective excitations can be described conveniently in terms of the nuclear response to an external perturbation, $V_{\rm ext} = \hat{Q}\, q^{\omega}_{\rm ext} e^{-i\omega t}$, with a vibration amplitude $q^{\omega}_{\rm ext}$ and the multipole one-body operator $\hat{Q} = r^L Y_{L0}(\theta)$ for $L \geqslant 2$ [1]. Its quantum average perturbation $\delta\langle\hat{Q}\rangle_t$ at time t is calculated through the Fourier transform as

$$\delta\langle\hat{Q}\rangle_\omega = -\chi^{\rm coll}_{QQ}(\omega) q^{\omega}_{\rm ext}\,, \tag{1}$$

where $\chi^{\rm coll}_{QQ}(\omega)$ is the collective response function [1,4]. The Hamiltonian at $q^{\omega}_{\rm ext} = 0$ depends on a collective variable q defined as the time-dependent deformation parameter of a mean-field potential $V(q)$ of the nucleus. The vibrations of the axially symmetric nuclear surface with a multipolarity L near the spherical shape can be described by $R(\theta, q) = R[1 + q(t)Y_{L0}(\theta)]$, $q(t) = q_\omega e^{-i\omega t}$; in spherical coordinates, $Y_{L0}(\theta)$ is the spherical harmonics. (The unperturbed quantities in dynamical variations are zero in this case.) The consistency condition is written as

$$\delta\langle\hat{Q}\rangle_\omega = \kappa_{QQ}\, \delta q_\omega, \tag{2}$$

where κ_{QQ} is the coupling constant, see Appendix A. With the help of condition (2), the collective response [1]

$$\chi^{\rm coll}_{QQ}(\omega) = \kappa_{QQ} \frac{\chi_{QQ}(\omega)}{\chi_{QQ}(\omega) + \kappa_{QQ}} \tag{3}$$

is expressed in terms of the so-called intrinsic response function, $\chi_{QQ}(\omega)$, defined by

$$\delta\langle\hat{Q}\rangle_\omega = -\chi_{QQ}(\omega)\big(\delta q_\omega + q^{\omega}_{\rm ext}\big). \tag{4}$$

One dominating peak in the collective strength function

$$S(\omega) = \frac{1}{\pi}\, {\rm Im}\chi^{\rm coll}_{QQ}(\omega), \tag{5}$$

based on Eq. (3) at low excitation energies $\hbar\omega_L$, is assumed to be well enough separated from all other solutions of the secular equation $\chi_{QQ}(\omega) + \kappa_{QQ} = 0$ for $\omega = \omega_L$. [See more detailed explanations of this approach for the case of the single-particle operator $\hat{F} = (\partial V/\partial q)_{q=0}$ in Eq. (A1) and its applications to the nuclear collective dynamics in Refs. [4,23,24]]. In this case, the oscillator response function in the q mode, $\chi^{\rm coll}_{qq}(\omega)$, can be conveniently written in an inverted approximate form [4,23] as

$$\frac{1}{\chi^{\rm coll}_{qq}(\omega)} = \frac{1}{\chi_{qq}(\omega)} + \kappa_{FF} = -M_{FF}\omega^2 - i\gamma_{FF}\omega + C_{FF}, \tag{6}$$

where κ_{FF} is the coupling constant in the F mode [Eq. (A1)], and

$$\chi_{qq}(\omega) = \frac{\chi_{FF}(\omega)}{\kappa^2_{FF}} = \frac{\chi_{QQ}(\omega)}{\kappa^2_{QQ}}. \tag{7}$$

According to the consistency conditions (2) and (A1), we used in Eq. (7) the approximate transformations between the quantities defined in different variables F and Q, corresponding to the single-particle operators $\hat{F}$ and $\hat{Q}$. These transformations will be used for presentation of the results satisfying the consistency condition for variations of the nuclear potential and the particle density in suitable units. The inverse collective response function for low frequencies ω is approximated in Eq. (6) by the response function of a damped harmonic oscillator, $\chi^{\rm coll}_{qq}(\omega)$, with the stiffness of the nuclear free energy $\mathcal{F}$, $C_{FF} \approx C_{FF}(0) = (\partial^2\mathcal{F}/\partial q^2)_{q=0}$, and the friction γ_{FF} and the inertia M_{FF},

$$\begin{aligned} C_{FF} &= C_{QQ}\, \frac{\kappa^2_{FF}}{\kappa^2_{QQ}}, \\ \gamma_{FF} &= \gamma_{QQ}\, \frac{\kappa^2_{FF}}{k^2_{QQ}}, \\ M_{FF} &= M_{QQ}\, \frac{\kappa^2_{FF}}{\kappa^2_{QQ}}. \end{aligned} \tag{8}$$

The consistent transport coefficients C_{QQ}, γ_{QQ}, and M_{QQ} in variables Q are related to the auxiliary intrinsic parameters $C_{QQ}(0)$, $\gamma_{QQ}(0)$, and $M_{QQ}(0)$, as those of expansion of the intrinsic response function $\chi_{QQ}(\omega)$ in ω in the "zero-frequency limit", $\omega \to 0$, for a slow enough collective motion [4]; that is,

$$\begin{aligned} &\chi_{QQ}(\omega) = \chi_{QQ}(0) - i\gamma_{QQ}(0)\,\omega - M_{QQ}(0)\,\omega^2 + \cdots, \\ &\chi_{QQ}(0) = -\kappa_{QQ} - C_{QQ}(0). \end{aligned} \tag{9}$$

Thus, for the transport parameters of the oscillator ω dependence in Eqs. (6) and (8), one has

$$\begin{aligned} C_{QQ} &= [1 + C_{QQ}(0)/\chi_{QQ}(0)]C_{QQ}(0), \\ \gamma_{QQ} &= [1 + C_{QQ}(0)/\chi_{QQ}(0)]^2\gamma_{QQ}(0), \\ M_{QQ} &= [1 + C_{QQ}(0)/\chi_{QQ}(0)]^2\big[M_{QQ}(0) + \gamma^2_{QQ}(0)/\chi_{QQ}(0)\big]. \end{aligned} \tag{10}$$

The intrinsic response $\chi_{QQ}(\omega)$ in Eqs. (3), (4), and (7) can be expressed in terms of the one-body Green's function G [17,34] as

$$\begin{aligned} \chi_{QQ}(\omega) = \frac{d_s}{\pi} \int_0^\infty d\varepsilon\, n(\varepsilon) \int d\mathbf{r}_1 \int d\mathbf{r}_2 \hat{Q}(\mathbf{r}_1) \\ \times \hat{Q}(\mathbf{r}_2)\, {\rm Im}G(\mathbf{r}_1, \mathbf{r}_2, \varepsilon)[G^*(\mathbf{r}_1, \mathbf{r}_2, \varepsilon - \hbar\omega) \\ + G(\mathbf{r}_1, \mathbf{r}_2, \varepsilon + \hbar\omega)], \end{aligned} \tag{11}$$

where $n(\varepsilon)$ is the Fermi occupation number at energy ε for temperature T, $n(\varepsilon) = \{1 + \exp[(\varepsilon - \lambda)/T]\}^{-1}$, with the chemical potential $\lambda \approx \varepsilon_F$, where ε_F is the Fermi energy. The factor of d_s accounts for the spin-isospin degeneracy by neglecting differences between the neutron and the proton potential wells. For Green's function $G(\mathbf{r}_1, \mathbf{r}_2, \varepsilon)$, we use the energy spectral representation

$$G(\mathbf{r}_1, \mathbf{r}_2, \varepsilon) = \sum_i \frac{\psi_i(\mathbf{r}_1)\psi^*_i(\mathbf{r}_2)}{\varepsilon - \varepsilon_i + i\epsilon}, \tag{12}$$

where ε_i are eigenvalues, ψ_i are eigenfunctions, and $\epsilon \to +0$ in the quantum mean-field approximation (asterisk in Eqs. (11) and (12) means the complex conjugation).

With the help of Eq. (11), the intrinsic response function $\chi_{QQ}(\omega)$ in the "zero-frequency limit" of Eq. (9) ($\omega \to 0$) can be expressed in terms of Green's function G through the intrinsic parameters [4,23,34]

$$\gamma_{QQ}(0) = -i\left(\frac{\partial \chi_{QQ}(\omega)}{\partial \omega}\right)_{\omega=0} = \frac{d_s\hbar}{\pi}\int_0^\infty d\varepsilon\, n(\varepsilon)\int d\mathbf{r}_1\int d\mathbf{r}_2\ \hat{Q}(\mathbf{r}_1)\,\hat{Q}(\mathbf{r}_2) \times \frac{\partial}{\partial \varepsilon}\left[\mathrm{Im}\, G\,(\mathbf{r}_1,\mathbf{r}_2,\varepsilon)\right]^2, \tag{13}$$

$$M_{QQ}(0) = \frac{1}{2}\left(\frac{\partial^2 \chi_{QQ}(\omega)}{\partial \omega^2}\right)_{\omega=0} = \frac{d_s\hbar^2}{\pi}\int_0^\infty d\varepsilon\, n(\varepsilon)\int d\mathbf{r}_1\int d\mathbf{r}_2\,\hat{Q}(\mathbf{r}_1)\,\hat{Q}(\mathbf{r}_2) \times \mathrm{Im}\, G(\mathbf{r}_1,\mathbf{r}_2,\varepsilon)\,\frac{\partial^2}{\partial \varepsilon^2}\mathrm{Re}\, G(\mathbf{r}_1,\mathbf{r}_2,\varepsilon). \tag{14}$$

Using the spectral representation (12) for Green's function G, one reduces equivalently Eq. (14) to the well-known cranking model inertia in the mean-field limit ($\epsilon \to +0$), see, e.g., Ref. [4].

For the collective response function at low-lying excitation energies, Eq. (3), with help of Eqs. (6) and (7), one has

$$\chi^{\mathrm{coll}}_{QQ}(\omega) = \frac{\kappa^2_{QQ}}{-M_{FF}\omega^2 - i\gamma_{FF}\omega + C_{FF}}, \tag{15}$$

where the inertia M_{FF}, friction γ_{FF}, and stiffness C_{FF} are given by Eqs. (8), (10), (13), and (14). The coupling constant κ_{QQ} is defined by the consistency condition (2), see Appendix A. Thus, with the strength function $S_L(\omega)$ in Eqs. (5) and (15) for the first lowest peak, one can evaluate the probability distributions for excitations of the low-lying collective states as

$$S_{L,l} = \hbar^{l+1}\int_0^\infty d\omega\ \omega^l\ S_L(\omega), \quad l = 0, 1, \ldots. \tag{16}$$

III. SEMICLASSICAL APPROACH

The intrinsic response function $\chi_{QQ}(\omega)$ [Eq. (11)] can be found with the help of the semiclassical expansion of Green's function G derived by Gutzwiller [12,13] from the quantum path-integral propagator, that is,

$$G(\mathbf{r}_1,\mathbf{r}_2,\varepsilon) = \sum_\alpha G_\alpha(\mathbf{r}_1,\mathbf{r}_2,\varepsilon), \tag{17}$$

where

$$G_\alpha(\mathbf{r}_1,\mathbf{r}_2,\varepsilon) = -\frac{1}{2\pi\hbar^2}|\mathcal{J}_\alpha(\mathbf{p}_1,t_\alpha;\mathbf{r}_2,\varepsilon)|^{1/2} \times \exp\left[\frac{i}{\hbar}S_\alpha(\mathbf{r}_1,\mathbf{r}_2,\varepsilon) - \frac{i\pi}{2}\mu_\alpha\right]. \tag{18}$$

The index α covers all classical isolated paths inside the potential well which connect the two spatial points $\mathbf{r}_1$ and $\mathbf{r}_2$ for a given energy ε. S_α is the classical action along such a trajectory α, and μ_α denotes a phase related to the Maslov index through the number of caustic and turning points of the path α [12,15]. The Jacobian $\mathcal{J}_\alpha(\mathbf{p}_1,t_\alpha;\mathbf{r}_2,\varepsilon)$ for transformation from the initial momentum $\mathbf{p}_1$ and the time t_α of particle motion along the trajectory α to its final coordinate $\mathbf{r}_2$ and energy ε is derived in Ref. [24] for the infinitely deep spherical square-well potential by means of the techniques explained in Refs. [12,13,15].

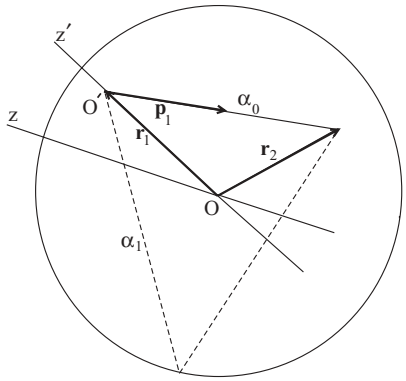

FIG. 1. Trajectory α_0 from the initial $\mathbf{r}_1$ to the final $\mathbf{r}_2$ point; the spherical coordinate systems with the polar axes z and z', the centers O and O', respectively, are shown; dashed line denotes another trajectory α_1 with one mirror reflection from the spherical boundary.

Among all classical trajectories α we may single out α_0 which directly connects $\mathbf{r}_1$ and $\mathbf{r}_2$ without reflections from the edge of potential well in intermediate points, see Fig. 1. For Green's function G [Eqs. (17) and (18)], one then has the separation $G = G_{\alpha 0} + G_{\mathrm{osc}}$, where $G_{\alpha 0}$ is given by Eq. (18) at $\alpha = \alpha_0$ and $G_{\mathrm{osc}}(\mathbf{r}_1,\mathbf{r}_2,\varepsilon)$ is coming from all other closed trajectories, $\alpha \neq \alpha_0$. It leads to the corresponding split of the semiclassical level density $g_{\mathrm{scl}}(\varepsilon)$, defined through the trace of G as

$$g_{\mathrm{scl}}(\varepsilon) = -\frac{1}{\pi}\mathrm{Im}\int d\mathbf{r}[G(\mathbf{r}_1,\mathbf{r}_2,\varepsilon)]_{\mathbf{r}_1\to\mathbf{r}_2\to\mathbf{r}} = g_{\mathrm{ETF}}(\varepsilon) + g_{\mathrm{osc}}(\varepsilon), \tag{19}$$

into a smooth part of the ETF model, $g_{\mathrm{ETF}}(\varepsilon)$, and its oscillating shell correction $g_{\mathrm{osc}}(\varepsilon)$ in terms of the POT sum over periodic orbits, see Refs. [12–15]. The ETF particle number conservation then becomes [12,14]

$$A = d_s\int_0^\infty d\varepsilon\, n(\varepsilon) g_{\mathrm{ETF}}(\varepsilon) = d_s\left[\frac{2(k_F R)^3}{9\pi} - \frac{(k_F R)^2}{4} + \frac{2k_F R}{3\pi}\right], \tag{20}$$

where k_F is the Fermi momentum in units of $\hbar$, $k_F = \sqrt{2m\varepsilon_F/\hbar^2}$, and m is the mass of the nucleon. Equation (20) determines the semiclassical parameter $k_F R$ as a function of the particle number A. The second and third terms in the very right approximation in Eq. (20) for spherical edgelike mean fields, which becomes exact for the infinitely deep square-well potential, account for important surface and curvature $\hbar$ corrections to the first main volume component, respectively. The temperature corrections $\sim(T/\varepsilon_F)^2$ might be taken into

account through the usual Sommerfeld expansion, too; see, for instance, Refs. [4,24]. We will omit such small corrections, because the applications will be related below to the low-lying collective excitations at zero temperature.

As is well known [12,15], due to $\hbar$ in the denominator of the exponent argument of Eq. (18) in the oscillating terms of Green's function traces, their semiclassical expansions in powers of $\hbar$ (or in the dimensionless parameter $\hbar/S_\alpha \sim 1/k_F R$) converge after averaging in $k_F R$, for instance, over a large enough interval of the particle number A through the radius R in accordance with Eq. (20). The Strutinsky averaging [9–11] with a Gaussian width Γ which covers at least a few gross shells in energy spectrum (see Appendix B) leads to the local ($\mathbf{r}_2 \to \mathbf{r}_1$) smooth quantities, in particular, to the level and the particle densities and the free energy. According to Eqs. (13) and (14), the nonlocal ($\mathbf{r}_2 \neq \mathbf{r}_1$) contributions into the ETF transport coefficients become also important. Therefore, we need more extended statistical averaging in the phase space (both energy and spatial coordinate) variables, as in the semiclassical (moreover, local hydrodynamical) derivations within the many-body particle density or Green's function formalism [8,28,35,36].

The averaged semiclassical inertia $\tilde{M}_{QQ}(0)$ and friction $\tilde{\gamma}_{QQ}(0)$ parameters can be found by substitution of the trajectory expansion of Green's function (17) into Eqs. (13) and (14),

$$\tilde{M}_{QQ}(0) = \frac{d_s\hbar^2}{\pi}\sum_{\alpha\alpha'}\Big\langle\int_0^\infty d\varepsilon\, n(\varepsilon)\int d\mathbf{r}_1\int d\mathbf{r}_2\hat{Q}(\mathbf{r}_1)\hat{Q}(\mathbf{r}_2) \times \mathrm{Im}\, G_\alpha(\mathbf{r}_1,\mathbf{r}_2,\varepsilon)\frac{\partial^2}{\partial\varepsilon^2}\mathrm{Re}\, G_{\alpha'}(\mathbf{r}_1,\mathbf{r}_2,\varepsilon)\Big\rangle_{\mathrm{av}}, \quad (21)$$

$$\tilde{\gamma}_{QQ}(0) = \frac{d_s\hbar}{\pi}\sum_{\alpha\alpha'}\Big\langle\int_0^\infty d\varepsilon\, n(\varepsilon)\int d\mathbf{r}_1\int d\mathbf{r}_2\hat{Q}(\mathbf{r}_1)\hat{Q}(\mathbf{r}_2) \times \frac{\partial}{\partial\varepsilon}[\mathrm{Im}\, G_\alpha(\mathbf{r}_1,\mathbf{r}_2,\varepsilon)\ \mathrm{Im}\, G_{\alpha'}(\mathbf{r}_1,\mathbf{r}_2,\varepsilon)]\Big\rangle_{\mathrm{av}}. \quad (22)$$

The angle brackets $\langle\cdots\rangle_{\mathrm{av}}$ mean the SCM averaging over the phase-space coordinates, as mentioned above. To calculate analytically these quantities, we need to distinguish the two limit cases [24]: (i) the nearly local part, $S_\alpha(\mathbf{r}_1,\mathbf{r}_2,\varepsilon_F)/\hbar = k_F\mathcal{L}_\alpha \lesssim 1$, and (ii) nonlocal contributions, $k_F\mathcal{L}_\alpha \gg 1$, where $\mathcal{L}_\alpha$ is the length of the trajectory α in the edgelike potential wells. We emphasize that the averaging over phase-space variables leads to the nearly local approximation (i) for the inertia [Eq. (21)] and the friction [Eq. (22)] coefficients, in contrast to the restriction (ii). For case (i), the partial SCM averaging in $k_F R$ (for instance, in nuclear sizes R or particle numbers A for constant k_F fixed by the particle density of the infinite matter, $\rho_\infty = 2k_F^3/3\pi^2$ [2]) ensures a convergence of the semiclassical expansions of smooth quantities in $1/k_F R$ within the ETF model [9,12,15]. The strong energy dependence of the exponential factor in Eq. (18), $\exp(iS_\alpha(\varepsilon)/\hbar)$, for $\hbar \to 0$, leads to the appearance of the damping factor, $\propto \exp[-(\mathcal{L}_\alpha\Gamma/4R)^2]$, after such averaging with a width of the Gaussian weight function, $\Gamma \approx (2\text{–}4)k_F R\hbar\Omega/2\varepsilon_F$; see Appendix B. This averaging which corresponds approximately to the 2–4 distances between the gross shells in the energy spectrum, $\hbar\Omega \approx \varepsilon_F/A^{1/3} = 7\text{–}10$ MeV, for heavy nuclei, $A = 200 - 50$, respectively, removes shell effects, almost like in the ETF level and particle densities [9–12,24]. The most important contribution is coming then from the shortest trajectory, $\alpha = \alpha' = \alpha_0$ (see Fig. 1), with a length s smaller or of the order of the wave length $1/k_F$, $\mathcal{L}_{\alpha 0} = s = |\mathbf{r}_2 - \mathbf{r}_1| \lesssim 1/k_F \ll R$, at a sufficiently large semiclassical parameter, $k_F R \gg 1$.

As in Refs. [24,28,36], it is convenient now to transform the variables $\{\mathbf{r}_1, \mathbf{r}_2\}$ to the Wigner coordinates $\{\mathbf{r}, \mathbf{s}\}$,

$$\mathbf{r} = \frac{\mathbf{r}_1 + \mathbf{r}_2}{2}, \quad \mathbf{s} = \mathbf{r}_2 - \mathbf{r}_1, \quad (23)$$

in order to simplify calculations of the inertia $\tilde{M}_{QQ}(0)$ [Eq. (21)] and the friction $\tilde{\gamma}_{QQ}(0)$ [Eq. (22)] by separating a smooth slow motion of particles in variable $\mathbf{r}$ and their fast dynamics in $\mathbf{s}$. As shown in Ref. [24], for small enough length s of the trajectory α_0, $s/R \ll 1$ within the nearly local approximation (i), the corresponding component $G_{\alpha 0}$ of Green's function (17) in Eqs. (21) and (22) in terms of the new integration variables $\{\mathbf{r}, \mathbf{s}\}$ is reduced approximately to its simple analytical form

$$G_{\alpha 0}(\mathbf{r}_1,\mathbf{r}_2,\varepsilon) \approx G_0(\mathbf{r}_1,\mathbf{r}_2,\varepsilon) = -\frac{m}{2\pi\hbar^2 s}\exp(iks), \quad s = |\mathbf{r}_2 - \mathbf{r}_1|, \quad (24)$$

with $k = \sqrt{2m\varepsilon/\hbar^2}$. Formally, G_0 coincides with the well-known Green's function for free particle motion [14,15,19,20]. With the transformation (23) and exchange of the energy and spatial integrations in Eqs. (21) and (22), in case (i), one has

$$\tilde{M}_{QQ}(0) = \frac{d_s\hbar^2}{\pi}\Big\langle\int d\mathbf{r}\int d\mathbf{s}\,\hat{Q}\left(\mathbf{r}+\frac{\mathbf{s}}{2}\right)\hat{Q}\left(\mathbf{r}-\frac{\mathbf{s}}{2}\right) \times \int_0^\infty d\varepsilon\, n(\varepsilon)\,\mathrm{Im}\, G_0\left(\mathbf{r}+\frac{\mathbf{s}}{2},\mathbf{r}-\frac{\mathbf{s}}{2},\varepsilon\right) \times \frac{\partial^2}{\partial\varepsilon^2}\mathrm{Re}\, G_0\left(\mathbf{r}+\frac{\mathbf{s}}{2},\mathbf{r}-\frac{\mathbf{s}}{2},\varepsilon\right)\Big\rangle_{\mathrm{av}}, \quad (25)$$

$$\tilde{\gamma}_{QQ}(0) = \frac{d_s\hbar}{\pi}\Big\langle\int d\mathbf{r}\int d\mathbf{s}\,\hat{Q}\left(\mathbf{r}+\frac{\mathbf{s}}{2}\right)\hat{Q}\left(\mathbf{r}-\frac{\mathbf{s}}{2}\right) \times \int_0^\infty d\varepsilon\, n(\varepsilon)\frac{\partial}{\partial\varepsilon}\left[\mathrm{Im}\, G_0\left(\mathbf{r}+\frac{\mathbf{s}}{2},\mathbf{r}-\frac{\mathbf{s}}{2},\varepsilon\right)\right]^2\Big\rangle_{\mathrm{av}}. \quad (26)$$

The internal integral over ε in Eqs. (25) and (26) can be taken analytically. For the analytical evaluation of the integrals over the Wigner coordinates $\mathbf{r}$ and $\mathbf{s}$, the integrands depending on $k_F s$ in Eqs. (25) and (26) are simplified by means of averaging in the phase-space variables. As demonstrated in Appendices B–D, using the approximation (24), one may identically transform the expressions for the inertia $\tilde{M}_{QQ}(0)$ and the friction $\tilde{\gamma}_{QQ}(0)$ and the isolated susceptibility $\tilde{\chi}_{QQ}(0)$ to sums of the local (volume) terms and their small nonlocal (surface) corrections. The integrands, proportional linearly to the nonlocal (correlationlike) components depending on $k_F R$, are zeros within approach (i). The inertia terms expressed linearly through the correlation function $\langle\hat{Q}(\mathbf{r}+\mathbf{s}/2)\hat{Q}(\mathbf{r}-\mathbf{s}/2) - \hat{Q}^2(\mathbf{r})\rangle_{\mathrm{av}}$, averaged in phase-space variables, are neglected as in the derivations of the hydrodynamic model

starting from a many-body system of strongly interacting particles [8,35]. The more general statistical principle of the weakness of correlations is used usually in semiclassical derivations of the kinetic equations with integral collision terms, by separating a slow motion along the mean coordinate **r** within the nearly local condition (i) from fast dynamics in the relative coordinate **s** in terms of its collisional correlations [28,36]. Such correlationlike functions are concentrated at small s of the order of a few wave lengths, as explained in Appendix B. The transport coefficients are simplified by doing averaging in fast oscillations of functions of the relative variable **s** at a given mean coordinate **r**. The integrations over angles of vectors **s** and **r** can be approximately performed analytically in the nearly local approximation (i), see Appendix B for details.

The major terms of Eqs. (25) and (26) can be found in the perfect local case when a smooth product of the multipole operators in these equations can be approximately taken off the integral over **s** at $\mathbf{s} = 0$ due to the property of the phase-space averaging of the correlation functions mentioned above. For the main local approximation within the framework of (i), after the integration over ε (or corresponding kR), one may take also analytically the integrals over **s** and **r** in Eqs. (25) and (26). As the final result for $L \geqslant 2$, one finally arrives at the inertia

$$\tilde{M}_{QQ}(0) = \frac{d_s m^3 R^{2L+6}}{12\pi\hbar^4} f_L^{(3)}, \tag{27}$$

the friction

$$\tilde{\gamma}_{QQ}(0) = \frac{d_s m^2 R^{2L+4}}{2\pi^2\hbar^3} f_L^{(1)}, \tag{28}$$

and the isolated susceptibility

$$\tilde{\chi}_{QQ}(0) = \frac{d_s m R^{2L+2}\, k_F R}{2\pi^2\,\hbar^2} f_L^{(0)}. \tag{29}$$

Here, $f_L^{(n)}$ are the integrals over the dimensionless radial variable, that is,

$$f_L^{(n)} = \int_0^1 d\wp\, \wp^{2L+2}\, (\wp+1)^n, \qquad n = 0, 1, 2, \ldots, \quad \wp = r/R, \tag{30}$$

$$f_L^{(0)} = \frac{1}{2L+3}, \quad f_L^{(1)} = \frac{4L+7}{2(L+2)(2L+3)}, \quad f_L^{(3)} = \frac{(4L+9)[(4L+9)^2-7]}{4(L+2)(L+3)(2L+3)(2L+5)}. \tag{31}$$

The next higher order terms of expansion of the product of multipole operators in powers of the dimensionless variable s/R lead to some relatively small surface corrections, $\sim 1/k_F R$, at large particle number A. In particular, it is shown that the next order curvature corrections, $\sim 1/(k_F R)^2$, for a given large $k_F R$ can be neglected within the nearly local approximation (i). Notice, more important surface ($\sim 1/k_F R$) and curvature [$\sim 1/(k_F R)^2$] corrections originate from those of the ETF relationship [Eq. (20)] between $k_F R$ and particle number A. The derivation of the surface and curvature corrections are considered in all Appendices. (They will be shown for brevity only at the very end of Sec. IV and will be discussed in Secs. V–VII).

For evaluation of the contributions (ii) of longer trajectories, the Gutzwiller expansion [Eqs. (17) and (18)], valid for the *isolated* classical paths, fails because we have to account for *a continuous symmetry* of the spherical Hamiltonian, i.e., the appearance of the axially symmetric degenerated families of planar periodic orbits with their points fixed inside of the spherical reflection boundary [15]. For such a family, due to the integration over its continuous parameter, the amplitude of G_α in expansion (17) of Green's function over trajectories α is enhanced on the order of $(k_F \mathcal{L}_\alpha)^{1/2}$ (or $\hbar^{-1/2}$, $k_F \mathcal{L}_\alpha \gg 1$), as compared to Eqs. (17) and (18), see Eqs. (16) and (31) in Ref. [15]. For the nondiagonal ($\alpha \neq \alpha'$) contributions (ii) into the integrals over $\mathbf{r}_2$ (or **s** in the **r** and **s** coordinates) in Eqs. (21) and (22) with parameter Γ of the SCM averaging [9] (much smaller than that related to the distance between gross shells $\hbar\Omega$), the leading terms in the semiclassical parameter $k_F R$ are the periodic orbits, according to the stationary-phase conditions [17]. The nondiagonal ($\alpha \neq \alpha'$) terms of Eqs. (21) and (22) through the stationary-phase (periodic-orbit) conditions provide mainly the shell (nonlocal) corrections to the inertia $M_{QQ}(0)$, friction $\gamma_{QQ}(0)$, and isolated susceptibility $\chi_{QQ}(0)$ [9]. They will be discussed in detail in further publications. In the following, we will consider only the smooth transport coefficients, and therefore, the tilde above them will be omitted for simplicity.

IV. COUPLING CONSTANTS AND TRANSPORT COEFFICIENTS

The consistent collective-transport coefficients γ_{QQ}, M_{QQ}, and C_{QQ} of Eq. (10) differ from their intrinsic parameters $\gamma_{QQ}(0)$ [Eq. (28)], $M_{QQ}(0)$ [Eq. (27)], and $C_{QQ}(0)$, see also $\chi_{QQ}(0)$ [Eq. (29)], in the low frequency expansion (9) by semiclassically small corrections,

$$\frac{C_{QQ}(0)}{\chi_{QQ}(0)} = \frac{C_{FF}(0)}{\chi_{FF}(0)} \sim \frac{1}{(k_F R)^2} \ll 1, \tag{32}$$

as shown in Refs. [4,24], and

$$\frac{\gamma_{QQ}^2(0)}{\chi_{QQ}(0) M_{QQ}(0)} = \frac{6}{\pi} \frac{\left[f_L^{(1)}\right]^2}{f_L^{(0)}\, f_L^{(3)}} \frac{1}{k_F R} \approx \frac{1}{k_F R} \ll 1, \tag{33}$$

in contrast to the corresponding result within the approach of Ref. [24]. Therefore, in the following derivations, we may neglect the corrections of Eq. (32) in Eq. (10) but keep Eq. (33) for the surface corrections, $\sim 1/k_F R$. Thus, up to relatively small surface corrections to the transport coefficients, one gets $\gamma_{QQ} \approx \gamma_{QQ}(0)$, $M_{QQ} \approx M_{QQ}(0)$, and $C_{QQ} \approx C_{QQ}(0)$.

For calculations of the response function $\chi_{QQ}^{\rm coll}(\omega)$ [Eq. (15)], one has to transform the transport coefficients γ_{QQ}, M_{QQ}, and C_{QQ} from the variable Q related to the one-body operator $\hat{Q}$ to another variable associated with the operator $\hat{F}$ by using Eq. (8) [1,4,24,34]. As shown in Appendix A, the coupling constants κ_{FF} and κ_{QQ} appearing in the transformations of

Eq. (8) are given by

$$\kappa_{FF} = -\frac{32\rho b_v K R^4}{675 b_s r_0} \approx -\frac{8\ KR}{225\pi\ b_s r_0}\ b_v A, \tag{34}$$

and

$$\kappa_{QQ} = \rho R^{L+3}, \quad \rho = \rho_\infty \left(1 + \frac{6 b_s r_0}{K R}\right) \approx \rho_\infty. \tag{35}$$

Here b_v is the energy of particle separation from nuclear matter, $b_v = 16$ MeV; K is the incompressibility modulus, $K = 220$ MeV; b_s is the energy surface constant, $b_s = 18$ MeV; and $r_0 = (3/4\pi\rho_\infty)^{1/3}$, where $\rho_\infty = 0.16$ fm^{-3} for the nuclear-matter particle density. For these typical nuclear parameters, the surface-tension particle-density correction in Eq. (35) inside of the nucleus is relatively small for heavy enough nuclei, i.e., $6 b_s r_0/KR \approx 6 b_s/K A^{1/3} \ll 1$, in the effective nuclear surface (ENS) approximation [25,26].

Substituting Eqs. (10), (34), (35), (27), and (28) into Eq. (8) for the consistent transport coefficients in the Thomas-Fermi approach, one approximately finds

$$M_{FF} = 6\pi^2 L f_L^{(3)} \rho \left(\frac{16 b_v\ KR}{2025\varepsilon_F\ b_s r_0}\right)^2 \frac{(k_F R)^4}{A} M_{\rm irr}, \tag{36}$$

$$M_{\rm irr} = \frac{3AmR^2}{4L\pi},$$

$$\gamma_{FF} = \frac{1}{2}\ f_L^{(1)} \left(\frac{32 b_v K R}{675\varepsilon_F b_s r_0}\right)^2 \gamma_{\rm wf}, \quad \gamma_{\rm wf} = \frac{3}{4}\hbar\rho k_F R^4, \tag{37}$$

where $M_{\rm irr}$ is the irrotational flow inertia of the hydrodynamic model [1], and $\gamma_{\rm wf}$ is the wall formula [18,20] derived in Ref. [24] for the operator $\hat{F}$ of Eq. (A1) in the same nearly local approximation (i). They both are used as convenient units. The incompressibility K and surface energy constant b_s appear in these equations in terms of the single semiclassical and leptodermic parameter $1/k_F R \sim a/R \propto b_s/K A^{1/3}$ ($k_F a \sim k_F r_0 \sim 1$, $R = r_0 A^{1/3}$) up to a number constant of the order of unity through Eq. (34) for the coupling constant κ_{FF}, see Appendix A. Such general common properties of the extended Thomas-Fermi and liquid drop models both based on expansion in this small parameter were found, for instance, within the ENS approach [25,26]. The ETF inertia M_{FF} in Eq. (36) is much larger than that of irrotational flow, $M_{\rm irr}$, for large enough particle numbers A when using the nuclear data mentioned above, that is,

$$\frac{M_{FF}}{M_{\rm irr}} = \overline{M}_{FF} A, \quad \overline{M}_{FF} \approx \left\{\begin{matrix} 0.036, & L = 2 \\ 0.043, & L = 3 \end{matrix}\right\}. \tag{38}$$

For $A = 100$–200, the inertia value M_{FF} [Eq. (38)] is larger than the irrotational flow one by a factor of about 4–7 for the quadrupole ($L = 2$) and almost 4–9 for the octupole ($L = 3$) vibrations (see Refs. [9,24] and also within another approach [37]).

Taking into account the nonlocal surface corrections in Eq. (B11) of Eq. (25) and in Eq. (33) of Eq. (10) [$\propto \gamma_{QQ}^2(0)$], which are both relatively small as $1/k_F R \sim A^{-1/3}$, for the inertia M_{FF} [see also Eq. (8)] up to the negligibly small curvature corrections of Eq. (32), one obtains

$$M_{FF} = \frac{\pi\rho m^3 R^{2L+6}}{2\hbar^4 k_F^3} \frac{\kappa_{FF}^2}{\kappa_{QQ}^2} \left(f_L^{(3)} + \frac{\zeta_L}{\pi\ k_F R}\right) \times \left(1 + \frac{6\left[f_L^{(1)}\right]^2}{\pi k_F R f_L^{(0)}\ f_L^{(3)}}\right). \tag{39}$$

Here, κ_{FF} and κ_{QQ} are the coupling constants (A8) and (A10) completed by surface and curvature corrections, respectively; $f_L^{(n)}$ are given by Eqs. (30) and (31), $\zeta_L = \zeta_L^{(1)} + \zeta_L^{(2)} > 0$; $\zeta_2^{(1)} = -3 f_2^{(2)} = -127/84$, $\zeta_2^{(2)} = 1279/576$ for $L = 2$; $\zeta_3^{(1)} = -3 f_3^{(2)} = -199/165$, $\zeta_3^{(2)} = 67031/42240$ at $L = 3$; and $f_L^{(2)} = (8L^2 + 32L + 31)/[(L+2)(2L+3)(2L+5)]$ [Eqs. (B10) and (B11)].

For the stiffness C_{FF} at leading order of expansion in $A^{-1/3}$ within the ENS approximation [24–26], as for the coupling constant κ_{FF}, one has the values of the hydrodynamic (HD) model for the vibration multipolarity L [1], i.e.,

$$C_{FF} \equiv C_L^{(S)} + C_L^{(\rm Coul)}. \tag{40}$$

The surface component of the HD stiffness,

$$C_L^{(S)} = \frac{b_s}{4\pi r_0^2}\ (L-1)(L+2)\ R^2, \tag{41}$$

is complemented by the Coulomb term along the β-stability line [1,38],

$$C_L^{(\rm Coul)} = -\frac{3\ (L-1)}{2\pi\ (2L+1)}\ \frac{Z^2 e^2}{R},$$

$$Z = \left[\frac{A}{2 + 3e^2\ A^{2/3}/5 r_0 b_{\rm sym}}\right], \tag{42}$$

where Ze is the charge of the nucleus. The square brackets in Eq. (42) mean the integer part of the number, and $b_{\rm sym}$ is the coefficient of the symmetry term in the nuclear binding energy, $b_{\rm sym} = 60$ MeV. The approximation $C_{FF} \approx C_{FF}(0)$ up to semiclassically small curvature corrections, $\sim A^{-2/3}$ [see Eq. (32)], was used here as in Eq. (39) [4,24].

V. VIBRATION ENERGIES AND SUM RULES

The energies of the collective vibration modes are determined by poles of the response function (15) with the inertia M_{FF} [Eq. (36)], friction γ_{FF} [Eq. (37)], and stiffness C_{FF} [Eq. (40)] as well as the coupling constant κ_{QQ} (35). These poles are given by

$$\omega_\pm = \varpi\left(\pm\sqrt{1-\eta^2} - i\eta\right), \tag{43}$$

where

$$\varpi = \sqrt{\frac{C_{FF}}{M_{FF}}}, \quad \eta = \frac{\gamma_{FF}}{2\sqrt{M_{FF}\ C_{FF}}}. \tag{44}$$

According to Eqs. (44), (37), (36), and (40), for the effective damping parameter η, one finds respectively $\eta \lesssim 0.4$ and 0.2 for $L = 2$ and 3. The last estimates were obtained for the same nuclear parameters shown above at $A \lesssim 200$ while

accounting for the surface and curvature corrections. As seen from these estimates, the collective motion under consideration is essentially underdamped, $\eta < 1$, for any particle number $A \lesssim 200$. Note that the residue interaction was zero from the very beginning in Eq. (12) for Green's function $G, \epsilon = +0$. The averaging over $k_F R$ (which guarantees a convergence of smooth transport coefficients in the semiclassical expansion in $1/k_F R$) leads to a finite friction coefficient γ_{FF} or an effective damping constant η, as formally, with the Lorentzian weight function [14,20] because of the appearance of a finite $\epsilon \neq 0$ in Eq. (12). However, as shown in this and the next two sections, the influence of an effective damping parameter η on calculations of the excitation energies, transitions probabilities, and EWSR contributions can be neglected in the following derivations.

Neglecting now the small η^2 term in the real part of Eq. (43) for calculations of the smooth low-lying collective vibration energy, $\hbar\omega = \hbar\,\mathrm{Re}\omega_+ \approx \hbar\varpi$, from Eqs. (43), (44), (36), and (40) ($L \geqslant 2$), one approximately obtains

$$\hbar\omega_L = \frac{\mathcal{D}_L}{A}, \quad \mathcal{D}_L = \overline{\mathcal{D}}_L \left(1 + \frac{C_L^{(\mathrm{Coul})}}{C_L^{(S)}}\right)^{1/2}, \tag{45}$$

$$\overline{\mathcal{D}}_L = \frac{75\, b_s \varepsilon_F}{4\pi b_v K} \sqrt{\frac{3\varepsilon_F b_s (L-1)(L+2)}{f_L^{(3)}}}. \tag{46}$$

For the nuclear parameters mentioned above, the constant $\overline{\mathcal{D}}_L$ independent of the particle number A is given approximately by $\overline{\mathcal{D}}_2 = 100$ MeV and $\overline{\mathcal{D}}_3 = 180$ MeV. With the Coulomb corrections of Eq. (45), these constants become slightly, almost linearly, decreasing functions of A within the interval of about $A = 100$–200. For this A interval, they are modified approximately to the values $\mathcal{D}_2 = 90$–70 and $\mathcal{D}_3 = 170$–150 MeV [see Eqs. (41) and (42)].

We may now evaluate the energy-weighted sum rule $S_{L,1}$ for the contribution of the first low-lying excitation, see the integral (16) at $l = 1$ with the strength function $S_L(\omega)$ [Eqs. (5) and (15)]. Finally, integrating analytically over ω in Eq. (16) for the EWSR of the low-lying collective excitation, one finds [see also Eqs. (16), (35), and (36)]

$$S_{L,1} = \frac{\hbar^2 \kappa_{QQ}^2}{2M_{FF}} = \frac{M_{\mathrm{irr}}}{M_{FF}} S_{L,\mathrm{cl}}, \tag{47}$$

where $S_{L,\mathrm{cl}}$ is the contribution of the low-lying peak in the hydrodynamic model of irrotational flow in a classical liquid drop, that is,

$$S_{L,\mathrm{cl}} = \frac{\hbar^2 \kappa_{QQ}^2}{2M_{\mathrm{irr}}} = \frac{3L\,\varepsilon_F}{4\pi\,(k_F R)^2}\, AR^{2L}. \tag{48}$$

This $S_{L,\mathrm{cl}}$ appears to be equivalent to the EWSR estimation independent of the model, see Eq. (6.179a) in Ref. [1]. The ratio of the inertias, M_{irr}/M_{FF}, in Eq. (47) is given by Eq. (36). Note that the last equation in Eq. (47) recalls the EWSR relation (6.183) of Ref. [1]. Thus, we may evaluate the relative contribution of the low-lying collective state into the total EWSR estimation (48) [see Eqs. (47), (36), and (38)],

$$\frac{S_{L,1}}{S_{L,\mathrm{cl}}} = \frac{\overline{\mathcal{S}}_L}{A}, \quad \overline{\mathcal{S}}_L = \frac{2}{L f_L^{(3)}} \left(\frac{225\varepsilon_F b_s k_F r_0}{8\pi b_v K}\right)^2, \tag{49}$$

with constants $\overline{\mathcal{S}}_2 \approx 7$ and $\overline{\mathcal{S}}_3 \approx 6$ for the same nuclear parameters. For $A \sim 100$–200, one has a relatively small EWSR contribution of the low-lying collective excitations in the framework of the Thomas-Fermi (TF) model. According to Eq. (38), this is obviously because of small enough values of the ratio of inertia parameters, M_{irr}/M_{FF}, for large particle numbers A. It is in contrast to the HD model where the first low-lying peak exhausts erroneously 100% of the EWSR (48) [1]. For this reason, the TF approach to the collective nuclear vibrations is much improved with respect to the HD model: in addition to the low-lying collective states, one has a possibility for the giant multipole resonance contributions which mainly exhaust the EWSR.

The relatively small surface and curvature corrections can be taken into account in the vibration energies [Eq. (44)] and sum rules [Eq. (47)] through Eq. (39) for the inertia and Eq. (20) for the ETF relationship of the parameter $k_F R$ to the particle number A [see Eqs. (A8) and (A10) and Appendix B]. The last kind of surface ($\sim A^{-1/3}$) and curvature ($\sim A^{-2/3}$) corrections from Eq. (20) give the major contribution to the A systematics of the vibration energies [Eq. (45)] for large A, that is,

$$\hbar\omega_L = \frac{\mathcal{D}_L}{A}\left(1 - \frac{w_L^{(s)}}{A^{1/3}} + \frac{w_L^{(c)}}{A^{2/3}}\right), \tag{50}$$

where $\mathcal{D}_L$ is defined in Eqs. (45) and (46),

$$w_L^{(s)} = \left(\frac{9\pi}{8}\right)^{2/3} \approx 2.3, \quad w_L^{(c)} = 3\left(\frac{8}{9\pi}\right)^{2/3} \approx 1.3. \tag{51}$$

Similarly, from Eq. (47) one obtains the EWSR ratio

$$\frac{S_{L,1}}{S_{L,\mathrm{cl}}} = \frac{\overline{\mathcal{S}}_L}{A}\left(1 - \frac{2w_L^{(s)}}{A^{1/3}} + \frac{\left[w_L^{(s)}\right]^2 + 2w_L^{(c)}}{A^{2/3}}\right), \tag{52}$$

where $\overline{\mathcal{S}}_L$ is the constant independent of the particle number A in Eq. (49). Other surface and curvature components do not contribute much because of their smallness or mutual compensations. Notice that the surface corrections essentially decrease both the vibration energies $\hbar\omega_L$ [Eq. (50)] and the EWSR contributions $S_{L,1}$ [Eq. (52)] for sufficiently large particle numbers, $A = 100$–200, because of the positive sign of the dominating surface correction, $w_L^{(s)} > 0$.

VI. TRANSITION PROBABILITIES AND DIRECT RADIATION DECAY

The radiation decay of the low-lying collective states can be considered as a direct emission of the γ quantum from a nucleus with the semiclassical description of a charged system within our ETF model. A similar process was studied in Ref. [39] for the case of the direct radiation decay of isoscalar giant multipole resonances within the framework of the semiclassical description of a nuclear system by using the Landau-Vlasov approach with macroscopic boundary conditions [27]. For the probability of the transitions per unit of time with the electric radiation of the γ-quantum energy ε_γ

at the multipolarity L, one has [38]

$$W(EL, I_1 \to I_2) = \frac{8\pi(L+1)}{L[(2L+1)!!]^2\hbar}\left(\frac{\epsilon_\gamma}{\hbar c}\right)^{2L+1} B(EL, I_1 \to I_2). \quad (53)$$

Here, I_1 and I_2 are the spins of the initial and the final states, $B(EL, I_1 \to I_2)$ is the reduced probability,

$$B(EL, I_1 \to I_2) = \sum_{\mu M_2} |\langle I_2 M_2|\mathcal{M}(EL, \mu)|I_1 M_1\rangle|^2, \quad (54)$$

μ and M_2 are the projections of the γ-quantum spin L and the angular momentum of a final nuclear state I_2, respectively, and

$$\mathcal{M}(EL, \mu) = \frac{eZ}{A}\int d\mathbf{r}\,\rho(\mathbf{r})\, r^L Y_{L\mu}(\theta, \varphi). \quad (55)$$

The effective charge factor can be approximately put at unity for the isoscalar collective excitations with $L \geqslant 2$.

The reduced probability $B(EL, 0 \to L)$ of Eq. (54) can be evaluated through the zero ($l = 0$) moment $S_{L,0}$ of the strength function $S_L(\omega)$, see Eqs. (16), (5), and (15). Taking into account the conservation equations for the energy $\varepsilon_\gamma = \hbar\omega_L$, and the angular momentum $I_2 = L$ ($I_1 = 0$) in the direct nuclear γ decay [38,39] for the zero moment of Eq. (16), one obtains [Eqs. (37) and (40)]

$$S_{L,0} = \frac{\hbar\,\kappa_{QQ}^2}{2\pi M_{FF}\omega_L\sqrt{1-\eta^2}}\,\mathrm{arccot}\left[\frac{2\eta^2-1}{2\eta\sqrt{1-\eta^2}}\right] = \frac{\hbar\,\kappa_{QQ}^2}{2M_{FF}\,\omega_L}\left[1-\frac{2\eta}{\pi}+\mathcal{O}(\eta^2)\right], \quad (56)$$

where M_{FF}, κ_{QQ}, and η are given by Eqs. (39), (A10), and (44), respectively ($\eta < 1/\sqrt{2}$). As shown in Sec. V, all small η corrections of Eq. (56) can be really neglected for particle numbers $A \lesssim 200$ and multipolarities $L \geqslant 2$. The averaged probability $B(EL, 0 \to L)$ in Eq. (54) can be then approximated semiclassically within the ETF model as

$$B(EL, 0 \to L) \approx B_{\mathrm{scl}}(EL, 0 \to L) = (2L+1)\left(\frac{eZ}{A}\right)^2 S_{L,0} \approx (2L+1)\left(\frac{eZ}{A}\right)^2 \frac{\hbar\kappa_{QQ}^2}{2M_{FF}\,\omega_L}. \quad (57)$$

The degeneracy factor $2L+1$ was accounted for because of the additional summation over the projections M_2 of the final angular momentum $I_2 = L$ in Eqs. (54) and (55), as compared to the simplest multipole operator for the isoscalar excitations of A nucleons, $\int d\mathbf{r}\,\rho(\mathbf{r})r^L Y_{L0}(\theta)$, in the previous sections. The factor $(eZ/A)^2$ must be also taken into account in the last two equations in Eq. (57) [see Eqs. (54) and (55), and Eqs. (6.61) and (6.182) of Ref. [1]]. The semiclassical energy of the low-lying collective state, $\hbar\omega_L$, was derived in Sec. V [see the first equation in Eq. (44) and its approximations (45) and (50)]. Other denotations are the same as in the sum rule of Eq. (47). Thus, from comparison of the transition probability (57) and the EWSR (47) modified with the operator (55), one has the expected approximate relationship between the probability (57) and the corresponding sum rule [1,39]:

$$S_{L,\mathrm{scl}} \equiv (2L+1)\left(\frac{eZ}{A}\right)^2 S_{L\,1} = \hbar\omega_L B_{\mathrm{scl}}(EL, 0 \to L). \quad (58)$$

According to Eqs. (58), (47), (38), (45), and (42), the reduced probability $B(EL)$ (for example, for the radiation process $L \to 0$) in units of the single-particle estimation [38] is mainly written as

$$\frac{B_{\mathrm{scl}}(EL)}{B_{\mathrm{s.p.}}(EL)} \approx \frac{\hbar^2 L(3+L)^2}{6mr_0^2\mathcal{D}_L\overline{M}_{FF}}\left(\frac{Z}{A}\right)^2 A^{1/3}. \quad (59)$$

As seen from this simple evaluation, the particle dependence of the reduced probability $B_{\mathrm{scl}}(EL)$ divided by the factor $(Z/A)^2$ in the single-particle units is roughly proportional to a semiclassically large parameter $A^{1/3}$. Taking into account also the coefficient in front of the $A^{1/3}$ dependence [Eq. (59)], one obtains an even larger magnitude for this relative probability, $\approx$80–130 for the quadrupole and $\approx$80–90 for the octupole low-lying collective states at particle numbers $A = 100$–200. With the main surface and curvature corrections of Eqs. (52) and (50), owing to the dominating ones of the ETF relationship between $k_F R$ and A, these quantities diminish with respect to their local (volume) approximation, $\approx$50–70 for $L = 2$ and $\approx$50–60 for $L = 3$. Thus, in any case, the quadrupole and octupole electric transitions within the ETF model are the well-pronounced-enough collective excitations.

For the mean semiclassical lifetime with respect to the direct γ decay, one has

$$t_{L,\mathrm{scl}} = W_{\mathrm{scl}}^{-1}(EL, L \to 0) \propto \omega_L^{-(2L+1)} B_{\mathrm{scl}}^{-1}(EL, L \to 0) \propto (A/eZ)^2 A^{2(2L+1)/3}. \quad (60)$$

With the semiclassical ETF probability per unit of time $W_{\mathrm{scl}}(EL, L \to 0)$ [Eq. (53)] corresponding to the reduced probability $B_{\mathrm{scl}}(EL, L \to 0)$ [Eq. (57)], one obtains $t_{2,\mathrm{scl}} \approx$ 80–1100 and $t_{3,\mathrm{scl}} \approx (17$–$1100) \times 10^6$ ps for quadrupole and octupole low-lying collective vibration states within the same particle number interval. We accounted for the main surface and curvature corrections which increase significantly lifetimes $t_{L,\mathrm{scl}}$ [Eq. (60)]. In all these evaluations, one can neglect the corrections caused by the conversion processes, which become important for much smaller excitation energies.

VII. DISCUSSION

Figures 2 and 3 show the local Thomas-Fermi approach to the low-lying collective quadrupole $\hbar\omega_2$ and octupole $\hbar\omega_3$ excitation energies [see Eq. (45) with Eq. (40) for the stiffness C_{FF} and Eq. (36) for the inertia M_{FF}] without surface and curvature corrections, as compared with the experimental data [31] and [32], respectively; see also Ref. [33]. The almost spherical (even-even) nuclei with quadrupole deformations, $q_2 \lesssim 0.05$, are selected from these experimental data [24,33,40,41]. The TF results for smooth vibration energies are significantly improved with respect to the hydrodynamic (HD) behavior with the same stiffness C_{FF} [Eq. (40)] but irrotational flow inertia M_{irr} [Eq. (36)], especially for the quadrupole case.

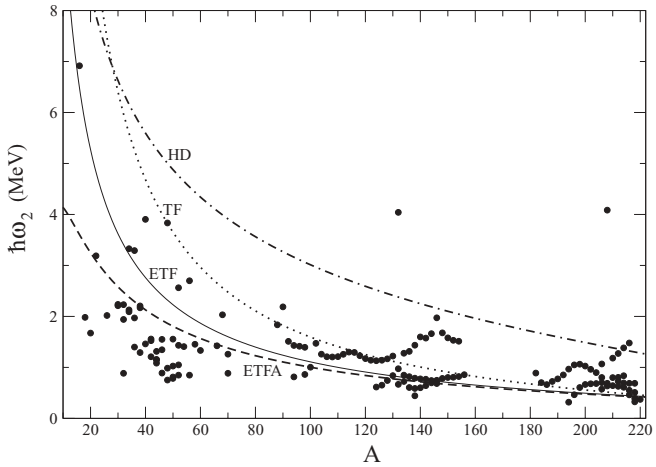

FIG. 2. Low-lying quadrupole vibration energies $\hbar\omega_2$ vs particle number A; curve TF is given by Eqs. (45), (44), (40), and (36); ETF is the extended TF approach accounting for the surface and curvature corrections of Eqs. (39) and (20); ETFA is the asymptotical formula (50) with Eq. (40) for the stiffness; and HD shows the standard hydrodynamical model [1]. Solid dots are the experimental data [31, 33] for the nearly spherical nuclei with quadrupole deformations $q_2 < 0.05$ [33,40,41]; $\rho = 0.16$ fm^{-3} ($r_0 = 1.14$ fm), $b_v = 16$ MeV, $b_s = 18$ MeV, $K = 220$ MeV, and $b_{\rm sym} = 60$ MeV.

The more complete ETF approach [Eqs. (45), (40) and (39)], which accounts for the surface and the curvature corrections of the function $k_F R(A)$, found from Eq. (20), and those of the inertia M_{FF}[Eqs. (39), (A8), and (A10)], is shown as ETF curves in Figs. 2 and 3. As expected, the comparison with experimental data, except for several doubly-closed-shell (magic) nuclei which appear above the regular A systematics, is essentially improved by these corrections mainly for smaller particle numbers A. The Coulomb stiffness component becomes important for larger A. The reason for the better agreement of the ETF approach, as compared to the HD model, with experimental data for nonmagic nuclei can be explained by larger ETF inertia M_{FF} [Eq. (38)] than that

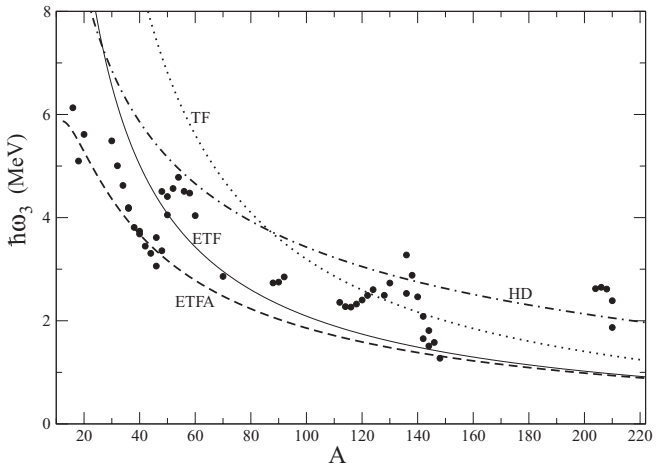

FIG. 3. Same as Fig. 2, but for the low-lying octupole vibration energies $\hbar\omega_3$; experimental data are from Refs. [32,33].

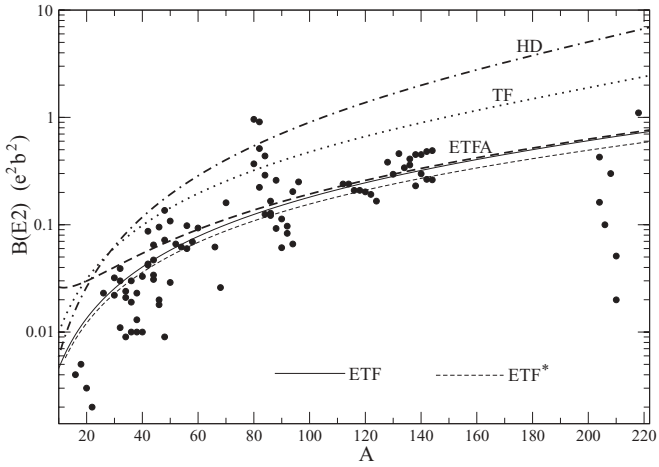

FIG. 4. Reduced probabilities $B(E2)$ for the transition $0^+ \to 2^+$ in units of e^2 b^2; solid dots are experimental data [31,33]; the semiclassical $B(E2)$ is given by Eq. (57) (short-dashed curve) with exact account for the η dependence and without η corrections (solid curve); other notation is the same as in Fig. 2.

of the irrotational flow $M_{\rm irr}$ for enough heavy nuclei. As seen from these figures, the explicitly analytical asymptotics of Eq. (50) (shown as ETFA), where only the surface and curvature corrections in the $k_F R(A)$ ETF dependence [Eq. (20)] were taken into account, are good asymptotics for $A \gtrsim 40$. This comparison shows the importance of these corrections, as compared to all other ones.

Figures 4 and 5 show the semiclassical reduced probability [$B_{\rm scl}(EL, 0 \to L) = (2L+1)B_{\rm scl}(EL, L \to 0)$, Eq. (57)] related to the zero ($l = 0$) moment [Eq. (16)] of the strength function in Eqs. (5) and (15) versus experimental data [31–33] for the quadrupole, $0^+ \to 2^+$, and the octupole, $0^+ \to 3^-$, electric collective transitions in the low-lying energy region for the same (almost spherical) nuclei. The logarithmic scale is used to show this comparison in a wide region of particle numbers. As displayed in these figures, one has a rather

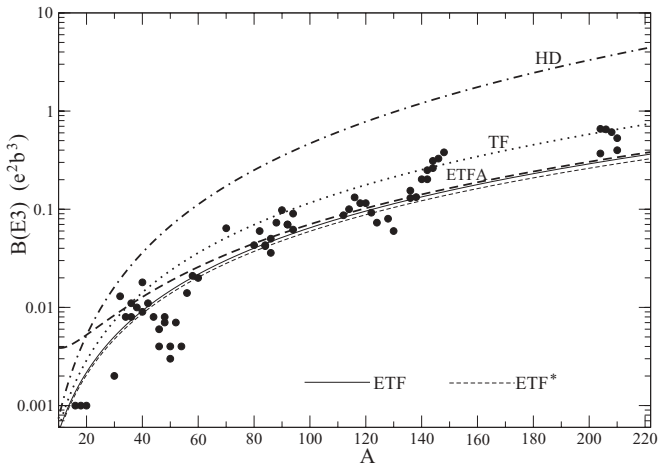

FIG. 5. Reduced transition probabilities $B(E3)$ for the transition $0^+ \to 3^-$ in units of e^2 b^3; notation is the same as in Fig. 4, but experimental data are from Refs. [32,33].

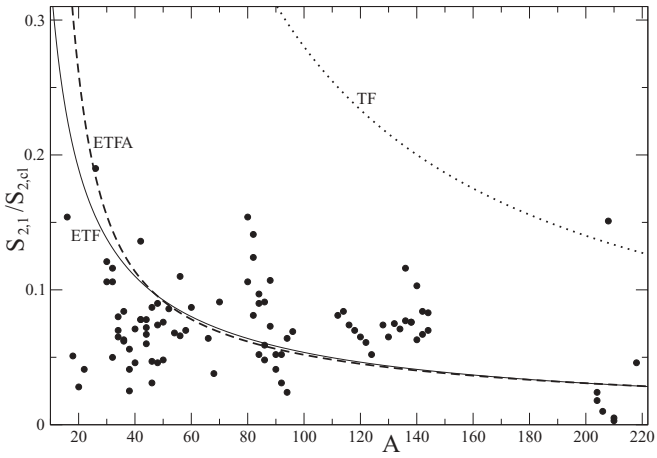

FIG. 6. Quadrupole EWSR $S_{2,1}$ of Eq. (16) in units of $S_{2,cl}$ from Eq. (48) [1]; solid data points show $\hbar\omega_2 B(E2)$ with the experimental vibration energies $\hbar\omega_2$ and reduced probabilities $B(E2)$ of Refs. [31, 33], see Figs. 2 and 4; the semiclassical $S_{2,1}$ is given by Eq. (47).

good agreement between the averaged semiclassical reduced transition probabilities [in particular, the lifetimes in Eq. (60)] and the global behavior of experimental data [31,32] (besides that of magic nuclei). The surface and the curvature correction effects measured by differences between TF and ETF curves greatly improve our semiclassical smooth A-systematic results toward the allowance data. The agreement between the full ETF (thin solid) and the analytical asymptotics ETFA (thick dashed) with the dominating surface and curvature corrections coming from Eq. (20) is really perfect for almost all particle numbers, except for small particle-number region. As seen from comparison of the ETF* and ETF curves in Figs. 4 and 5, one may really neglect the η corrections of Eq. (57) which arise artificially from the averaging procedure.

One of the most important characteristics of the low-lying collective states is their energy-weighted sum rule contribution [Eq. (47)] into the total value of Eq. (48) [1], see Figs. 6 and 7. The experimental EWSR were evaluated as the products

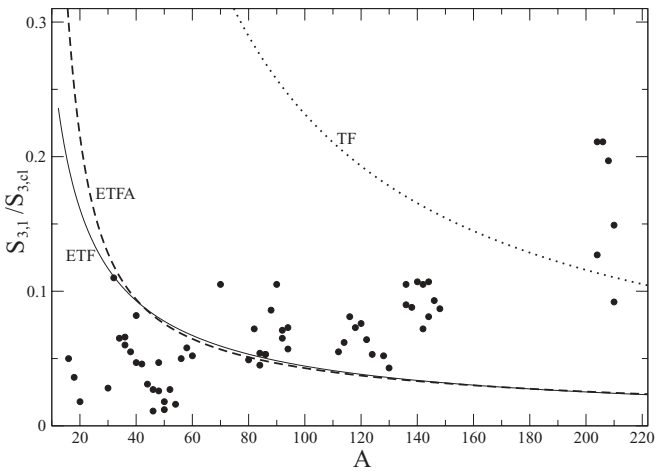

FIG. 7. Octupole EWSR $S_{3,1}$ in units of $S_{3,cl}$ [Eq. (48) [1]; data points show $\hbar\omega_3 B(E3)$ with the experimental $\hbar\omega_3$ and $B(E3)$ from Refs. [32,33]; other notation is the same as in Fig. 6.

of the measured transition probabilities $B(EL)$ plotted in Figs. 4 and 5 and the corresponding vibration energies $\hbar\omega_L$ (see Figs. 2 and 3) both taken from Refs. [31] and [32] for the quadrupole (Fig. 6) and octupole (Fig. 7) vibrations, respectively. According to Eqs. (38), by the same reason of enhancement of the inertia M_{FF} with respect to the irrotational flow M_{irr}, the relative contribution of the low-lying collective states into the EWSR within the TF approach [Eqs. (47) and (36)] and the more complete ETF model [Eqs. (47), (39), (A8), and (A10)] become basically correct for larger particle numbers A, in contrast to the HD model. As shown in Figs. 6 and 7, within the ETF approximation, we obtained relatively much smaller EWSR contributions of these states [see Eqs. (47), (52), and (51)] into the total EWSR [Eq. (48)] for large enough particle numbers, $A \gtrsim 70$. This is mainly in agreement with experimental data [31,32] for the EWSR at such values of A, especially better when accounting for the surface and the curvature corrections. Again, the good EWSR asymptotics of Eq. (52) (ETFA) for large A takes only into account the most essential surface and curvature corrections of the $k_F R(A)$ function as determined by the ETF particle number conservation equation (20).

However, Figs. 2–7 show also the obvious importance of other contributions, first of all arising from the shell effects, which are especially pronounced for the quadrupole case,[1] see Figs. 2, 4, 6. They are certainly beyond the smooth ETF approximation, in line of the SCM results of Ref. [9]. As expected, magic nuclei such as Pb-208 [the full point much above others on right of Figs. 2 and 6 and near the very right of the minimum of the $B(EL)$ in Fig. 4, for example] should be excluded from comparison with the ETF approach for vibration energies, the reduced transition probabilities, and the EWSR contributions. The deflection of the experimental data for $B(EL)$ from the averaged semiclassical A dependences can be assumed to be referred to those of the matrix elements in Eq. (54) within both of the more exact RPA and POT approaches, taking into account the shell effects. As noted in Refs. [9,24], the pairing effects in calculations of the inertia within the cranking model [5,11] for even-even nuclei, lead basically to the $A^{-2/3}$ behavior for both the not too heavy and light nuclei [40,41]. Notice that the mean vibration energy $\hbar\omega_L$ as function of its multipolarity L [Eqs. (45), (46), and (50)] differs essentially from that predicted by the hydrodynamical approach [1] and the pairing cranking model [5] and from that found in Ref. [24] (with the same surface HD stiffness) because of different evaluations of the inertia. For heavy nuclei, the A dependence of the pairing gap is more undetermined, and the pairing correlation effects are still a challenge to the investigation of smooth and shell components of the transport coefficients within the POT approximation to the SCM. Nevertheless, as seen from Figs. 2–7, the ETF approximation accounting for the Coulomb, surface,

[1]The smooth ETF energies $\hbar\omega_L$ of Eq. (44), probabilities $B(EL)$, and EWSR [Eqs. (16), (5), and (15)] differ from the statistically averaged experimental data [31,32] because originally, they depend on the oscillating shell components of the transport coefficients and coupling constants in a complicated nonlinear way [9].

and curvature corrections (even without pairing correlations) are largely in good agreement with the experimental data for the almost spherical heavy enough nuclei, except for enhancement due to the obviously pronounced shell effects in a few doubly-closed-shell nuclei.

VIII. CONCLUSIONS

For low-lying nuclear collective excitations within a few lowest orders of the POT in $\hbar$ corresponding to the extended Thomas-Fermi approximation, we derived smooth inertia for the vibrations near a spherical shape of the mean edgelike field. The consistent collective ETF inertia is significantly larger than that of irrotational flow. The smooth low-lying collective vibration energies in almost spherical (besides doubly-closed-shell) nuclei might roughly satisfy the A^{-1} particle-number dependence with the $A^{-1/3}$ surface and $A^{-2/3}$ curvature corrections for heavy enough nuclei, in contrast to the mainly $A^{-1/2}$ behavior predicted by the HD model and $A^{-1/3}$ dependence obtained in Ref. [24]. We emphasize the importance of the quantum $\hbar$ (surface) corrections (coming mainly from the ETF dependence of the semiclassical parameter $k_F R$ on particle number A) in comparison with experimental data for the quadrupole and octupole vibration energies and their EWSR contributions. As the ETF inertia M_{FF} is significantly larger than $M_{\rm irr}$ for the irrotational hydrodynamic flow, our vibration energies, the electric reduced transition probabilities, and contributions to the EWSR are basically in much better agreement with their experimental data than those found in the HD approach for large enough (nonmagic) particle numbers. We proved semiclassically that the reduced transition probabilities in Weisskopf units for the low-lying vibration excitations are sufficiently large to refer them to the collective states. The effect of surface corrections on the smooth vibration energies and the sum rules within the ETF approach is much emphasized in comparison with the TF approximation leading in semiclassical expansion over $1/k_F R$. We found simple analytical asymptotics for the vibration energies, the reduced probabilities, and the EWSR with explicit A dependence for larger particle numbers A in very good agreement with the more complete ETF approach. We point out also the importance of the shell effects in all such characteristics of low-lying collective states in magic nuclei, especially for the collective quadrupole-vibration modes which are certainly outside of the smooth A systematics predicted by the ETF model.

For further perspectives, the Gutzwiller trajectory expansion (17) which accounts for symmetries of the Hamiltonian [15] can be used in the semiclassical derivations of inertia and friction by applying the stationary-phase method for calculating the transport coefficients in order to study their shell corrections in terms of the periodic orbits [17]. This approach can be also applied to calculations of the moment of inertia for analysis of allowance data on the collective states in rotating nuclei; see Ref. [42] for the ETF step of their study. We hope to semiclassically overcome some problems with the inertia and friction calculations which take into account the dissipative width of the multipole strength functions.

ACKNOWLEDGMENTS

We are pleased to thank Profs. H. Hofmann, V. M. Kolomietz, V. A. Plujko, V. I. Abrosimov, and F. A. Ivanyuk, and Dr. O. M. Gorbachenko for many fruitful discussions and suggestions. We also gratefully acknowledge our colleagues V. A. Plujko and O. M. Gorbachenko for providing the files with experimental data on the low-lying vibration energies and multipole transition probabilities, which were prepared in accordance with Refs. [31,32]. A.G.M. acknowledges the Physical Department of the Technical Munich University for its very kind hospitality during his stay.

APPENDIX A: COUPLING CONSTANTS

The consistency condition for the single-particle operator $\hat{F}$ of the external field reads [1,4]

$$\delta\langle\hat{F}\rangle_\omega = \kappa_{FF}\,\delta q_\omega, \qquad \kappa_{FF} = -\chi_{FF}(0) - C_{FF}(0), \quad \hat{F} = \left(\frac{\partial V}{\partial q}\right)_{q=0}, \tag{A1}$$

where κ_{FF} is the coupling constant, and $\chi_{FF}(0)$ is the corresponding isolated susceptibility in the F mode. For a quasistatic process, the first consistency relation in Eq. (A1),

$$\delta\langle\hat{F}\rangle = \int d\mathbf{r}\hat{F}(\mathbf{r})\delta\rho(\mathbf{r},q) = \int d\mathbf{r}\hat{F}(\mathbf{r})\left(\frac{\partial\rho(\mathbf{r},q)}{\partial q}\right)_{q=0}\delta q, \tag{A2}$$

determines the coupling constant κ_{FF} by

$$\kappa_{FF} = \int d\mathbf{r}\,\hat{F}(\mathbf{r})\left(\frac{\partial\rho(\mathbf{r},q)}{\partial q}\right)_{q=0}. \tag{A3}$$

Within the considered macroscopic model, the particle density variation (transition density) can be presented as a sum of the "volume" and "surface" parts in the effective nuclear-surface (ENS) approximation [25,26]

$$\delta\rho(\mathbf{r},q) = \delta\rho_{\rm vol}(\mathbf{r},q)\; y(\xi) - \rho_{\rm in}\frac{R}{a}\,\frac{\partial y(\xi)}{\partial\xi}\,Y_{L0}(\hat{\mathbf{r}}). \tag{A4}$$

Here $\rho_{\rm in}$ [Eq. (35), low index in $\rho_{\rm in}$ is omitted in the main text] is the particle density inside of the system far from the ENS [the spatial points of maximal particle density gradient $\nabla\rho(\mathbf{r})$], $\hat{\mathbf{r}} = \mathbf{r}/r$. The radial coordinate dependence of the particle density, $\rho(r,\theta,q) = \rho_{\rm in}y(\xi)$, $\xi = [r - R(\theta,q)]/a$, is approximated via the profile steplike function $y(\xi)$ with a sharp change from 0 to 1 near the nuclear surface, $r = R(\theta,q)$, within a small transition region of the order of a diffuseness parameter, $a = (4\beta\rho_\infty/b_v)^{1/2}$. The coefficient β (in front of the $[\nabla\rho(r)]^2$ term of the effective nuclear Skyrme forces) is given by [26]

$$\beta = \frac{4\pi r_0^5\, b_s^2}{27 b_v\, J^2}, \quad J = \int_{-\infty}^{\xi_0} d\xi\left(\frac{dy(\xi)}{d\xi}\right)^2 \approx \frac{8}{15}, \qquad y(\xi) = \frac{\rho(\xi)}{\rho} \approx \tanh^2(\xi - \xi_0), \tag{A5}$$

where $\xi_0/R = \mathrm{arctanh}(\sqrt{y_0}) = 0.658\ldots$ for the value $y = y_0 = 1/3$ at the ENS, $b_s \approx 4b_v a/5r_0$. The solution $y(\xi)$ of (A5) for the particle density is related to the simplest parabolic approximation $-b_v + K(1-y)^2/18$ for the energy density per particle inside the nucleus up to a relatively small kinetic energy $[\nabla\rho(r)]^2$ correction in the ENS layer of the width a. As shown in Ref. [26], it is in good agreement with the Hartree-Fock calculations of the particle densities based on several Skyrme force parameters, except for small quantum effects outside of the narrow ENS layer.

In the framework of the ENS approximation, at leading order of expansion in the parameter $a/R \sim A^{-1/3}$, for the operator $\hat{F}(\mathbf{r})$ of Eq. (A1) ($L \geqslant 2$), one has

$$\hat{F}(\mathbf{r}) = \left(\frac{\delta V}{\delta\rho}\frac{\partial\rho(\mathbf{r},q)}{\partial q}\right)_{q=0} \approx -RY_{L0}(\hat{\mathbf{r}})\left(\frac{\delta V}{\delta\rho}\frac{\partial\rho}{\partial r}\right)_{q=0} = \frac{RK}{9\rho}Y_{L0}(\hat{\mathbf{r}})\left(\frac{\partial\rho}{\partial r}\right)_{q=0}, \tag{A6}$$

up to relatively small corrections of the order of $6b_s/KA^{1/3}$ to the "volume" particle density variations in Eq. (A4), see Eq. (35). To evaluate the variational derivative $\delta V/\delta\rho$ in Eq. (A6), we used the thermodynamical relation (energy conservation equation), $d\lambda = -\mathcal{S}\,dT + d\mathcal{P}/\rho + dV$, where $\mathcal{S}$ is the nuclear entropy, $\mathcal{P}$ the pressure, and V a quasistatic external field [4]. Then, the conservation of particle number at constant temperature T (constant chemical potential λ and $T \equiv 0$) and the definition of incompressibility, $K = 9(\partial\mathcal{P}/\partial\rho)_{q=0}$, were taken into account in the third equation of Eq. (A6). Substituting Eqs. (A6) and (A4) into (A3) and taking smooth r-dependent quantities, as compared to the sharp radial derivatives of particle density at $q = 0$ off the integral over r, we may use the ENS approximation for surface tension $b_s/4\pi r_0^2$ [25,26], i.e.,

$$b_s \approx 8\pi\beta r_0^2\int_0^\infty dr\left(\frac{\partial\rho(r)}{\partial r}\right)^2. \tag{A7}$$

With this expression for b_s, up to small terms of the relatively high order in $A^{-1/3}$ [in particular, those of Eq. (32)], and small "volume" particle density terms, $\sim(6b_s/KA^{1/3})^2$, one approximately obtains

$$\kappa_{FF} \approx -R\int d\mathbf{r}\hat{F}(\mathbf{r})\,Y_{L0}(\hat{\mathbf{r}})\left(\frac{\partial\rho}{\partial r}\right)_{q=0} = -\frac{Kb_sR^4}{72\pi\rho\beta r_0^2}, \tag{A8}$$

see Eq. (35) for the particle density ρ and Eq. (A5) for β. From Eqs. (A8) and (A5) for the coupling constant κ_{FF}, one arrives at Eq. (34).

Similarly, from the consistency condition (2), one may write

$$\delta\langle\hat{Q}\rangle = \int d\mathbf{r}\,\hat{Q}(\mathbf{r})\,\delta\rho(\mathbf{r},q) = \kappa_{QQ}\,\delta q, \tag{A9}$$

where $\delta\rho(\mathbf{r},q)$ is the particle density variation (A4) with the same edgelike function $y(\xi)$ described above. Up to negligibly small corrections in expansion over parameter a/R from Eqs. (A9) and (A4), one finds

$$\kappa_{QQ} = \rho R^{L+3}\left[1 + \left(\frac{\xi_0}{R} - 1\right)(L+2)\frac{a}{R} + (L+1)(L+2)\left(\frac{\xi_0^2}{2R^2} - \frac{\xi_0}{R} + \log 2\right)\frac{a^2}{R^2}\right]. \tag{A10}$$

In these derivations, the boundary condition for pressures of the ENS approach [25,26] was used to relate the slow volume and surface vibration amplitudes in Eq. (A4). The radial volume particle density dependence in (A4), $\delta\rho_{\mathrm{vol}}(\mathbf{r})$, is evaluated as in the macroscopic zero-sound Fermi-liquid models [26,28–30] for nuclear low-lying excitations. It leads to a negligibly small factor, $3(L-1)(L+2)b_s/(2L+3)KA^{1/3}$, as compared to the dominating surface term of the sum (A4). Other important corrections of Eq. (A10) were obtained from expansion of the integral of the surface part of the particle density variation in Eq. (A4) in the small parameter, $a/R \approx 5b_sr_0/4b_vR \approx 1.4/A^{1/3}$, at second (curvature) order. The analytical solution (A5) for $y(\xi)$ was explicitly used for the integrations over the radial variable in Eq. (A9). Up to relatively small volume corrections, $\sim b_s/KA^{1/3}$, and those of Eq. (A10), one obtains Eq. (35).

APPENDIX B: CALCULATIONS OF THE INERTIA

For the integration over $\mathbf{s}$ in Eq. (25) within the nearly local approximation (i), one may use the spherical coordinate system with the center O' at the point $\mathbf{r} \approx \mathbf{r}_1$ for a given $\mathbf{r}$ and the polar axis z', see Fig. 1. The integration over $\mathbf{r}$ can be performed in the usual spherical coordinate system with the symmetry center O and axis z shown in this figure too. The approximation (i) and these coordinate systems simplify the integration limits. Introducing the dimensionless variables $\wp = r/R$, $\sigma = s/R$, and $u = kR$, we subtract and add identically the same local part [Eq. (27)] with its nonlocal surface correction $\tilde{M}^{(0)}_{QQ}(0)$,

$$\tilde{M}^{(0)}_{QQ}(0) = \frac{\pi}{4}\left\langle\int_0^1 d\wp\,\wp^{2(L+1)}\int_0^{1+\wp} d\sigma\,\sigma^2\tilde{B}(u_F\sigma)\right\rangle_{\mathrm{av}}. \tag{B1}$$

Separating the correlationlike terms in the integrand of Eq. (25), one has

$$\tilde{M}_{QQ}(0) = \tilde{M}^{(0)}_{QQ}(0) + \tilde{M}^{(1)}_{QQ}(0) + \tilde{M}^{(2)}_{QQ}(0) + \tilde{M}^{(3)}_{QQ}(0), \tag{B2}$$

where

$$\tilde{M}^{(1)}_{QQ}(0) = \left\langle\int_0^1 d\wp\,\wp^{2(L+1)}\times\int_0^{1+\wp} d\sigma\,\sigma^2\,\Delta_Q(\wp,\sigma)\,\tilde{B}(u_F\sigma)\right\rangle_{\mathrm{av}}, \tag{B3}$$

$$\tilde{M}^{(2)}_{QQ}(0) = \left\langle\int_0^1 d\wp\,\wp^{2(L+1)}\times\int_0^{1+\wp} d\sigma\,\sigma^2\Delta_B(u_F\sigma)\right\rangle_{\mathrm{av}}, \tag{B4}$$

$$\tilde{M}^{(3)}_{QQ}(0) = \left\langle \int_0^1 d\wp\, \wp^{2(L+1)} \times \int_0^{1+\wp} d\sigma\, \sigma^2\, \Delta_Q(\wp,\sigma)\, \Delta_B(u_F\sigma) \right\rangle_{\rm av}. \quad \text{(B5)}$$

Here, we introduced several helpful functions. Namely,

$$\begin{aligned} B(w) &= \mathcal{I} \int_0^w dx\, \sin(x)\, j_1(x) \\ &= \frac{\mathcal{I}}{2}\left\{ \mathrm{Si}(w) - \frac{1}{w}[1-\cos(2w)] \right\} \\ &\to \mathcal{I}\left[\frac{\pi}{4} - \frac{1}{2w} + \frac{1}{4w}\cos(2w) \right. \\ &\quad \left. - \frac{1}{8w^2}\sin(2w) + \cdots \right], \end{aligned} \quad \text{(B6)}$$

with $w = k_F R\sigma$ and $\mathcal{I} = d_s m^3 R^{2L+6}/\pi^2\hbar^4$; $j_n(x)$ $(n = 0, 1, \ldots)$ is the spherical Bessel function, and $\mathrm{Si}(x)$ is the integral sine. The correlationlike functions denoted by Δ in Eqs. (B3)–(B5) are defined by $\Delta_B = B - \tilde{B}$ with the SCM energy spectrum averaging over $k_F R$, $\tilde{B}(u_F\sigma)$, and

$$\begin{aligned} \Delta_Q\left(\frac{\sigma}{\wp}\right) &= \frac{1}{4\pi r^{2L}} \int d\Omega \int d\Omega_s \left[\hat{Q}\left(\mathbf{r}+\frac{\mathbf{s}}{2}\right) \hat{Q}\left(\mathbf{r}-\frac{\mathbf{s}}{2}\right) \right. \\ &\quad \left. - r^{2L} Y^2_{L0}(\cos\theta) \right] \\ &= c_L^{(2)}\left(\frac{\sigma}{\wp}\right)^2 + c_L^{(4)}\left(\frac{\sigma}{\wp}\right)^4 + c_L^{(6)}\left(\frac{\sigma}{\wp}\right)^6 + \cdots, \end{aligned} \quad \text{(B7)}$$

where $c_2^{(2)} = -5/6$, $c_2^{(4)} = 1/16$, $c_2^{(n\geqslant 6)} = 0$ at $L = 2$, and $c_3^{(2)} = -7/4$, $c_3^{(4)} = 7/16$, $c_3^{(6)} = -1/64$, $c_3^{(n\geqslant 8)} = 0$ at $L = 3$, etc. The integrals (B7) were evaluated over all possible spherical angles of the vectors $\mathbf{r}$ and $\mathbf{s}$ in the nearly local approximation (i), where the only small $s/R \lesssim 1/k_F R$, give the leading contributions; $d\Omega = \sin\theta d\theta\, d\varphi$, and $d\Omega_s = \sin\theta_s\, d\theta_s d\varphi_s$. The integration over the modulus of vector $\mathbf{s}$ was extended approximately to the maximal one for a given $r \approx r_1$. Then, we integrated over all such modules of vector $\mathbf{r}$ within the approximation mentioned above.

The phase-space averaging in Eqs. (B1)–(B5) are exchanged with the integrations over the spatial coordinates. For calculations of the inertia component $\tilde{M}_{QQ}(0)$ [Eq. (25)], the function $B(k_F R\sigma)$ in Eq. (B6) (shown in Fig. 8) can be expanded in the small semiclassical parameter $1/k_F R$; see the asymptotics in Eq. (B6) for large arguments. As seen from this asymptotics, its oscillating terms are removed by Strutinsky averaging in $u_F = k_F R$ [9–12,24],

$$B_\Gamma(u_F\sigma) = \int_{-\infty}^{\infty} dx\, B[(u_F + x\Gamma)\sigma](1 + x\Gamma/u_F)^{2(L+3)} \times f_{\rm av}^{(2\nu)}(x), \quad f_{\rm av}^{(2\nu)}(x) = \frac{1}{\sqrt{\pi}}\, e^{-x^2} P_{2\nu}(x). \quad \text{(B8)}$$

The correction polynomial of the order of 2ν, $P_{2\nu}(x) = \sum_{\tau=0,2,\ldots}^{2\nu} v_\tau H_\tau(x)$, is defined through the recurrence relations $v_\tau = -v_{\tau-2}/2\tau$ and $v_0 = 1$; $H_\tau(x)$ is the standard Hermite polynomial. The second multiplier in the integrand of Eq. (B8) takes into account that we average really in R [or particle number A, according to Eq. (20)] in variable $k_F R$ for a fixed k_F by the phenomenological value of the infinite-matter particle density; see the main text after Eq. (22). Figure 9 shows a study of the so-called plateau condition for the averaged function $B_\Gamma(u_F\sigma)$ from Eq. (B8) at several small enough $\sigma = s/R$, i.e., the condition that the value $\tilde{B}$ of $B_\Gamma(u_F\sigma)$ is almost independent of the Gaussian width Γ and the correction polynomial degree 2ν in the SCM procedure within their rather wide intervals, $\Gamma \approx 1$–3 and $2\nu \approx 6, 8$.

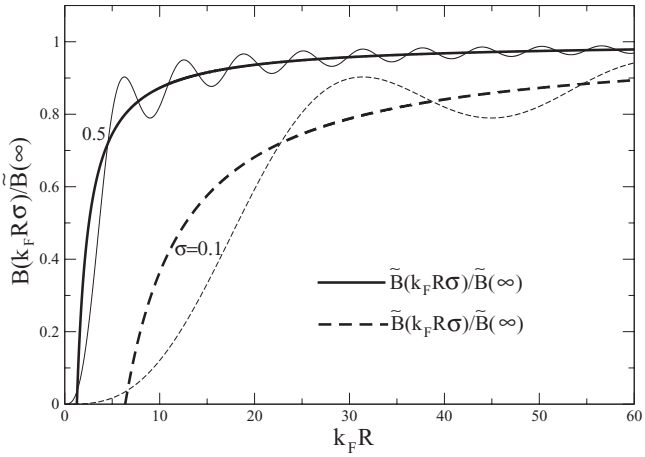

FIG. 8. Function $B(k_F R\sigma)$ of Eq. (B6) (short-dashed and thin solid lines) in units of asymptotic constant $\tilde{B}(\infty)$ at the two characteristic values of $\sigma = s/R = 0.1$ and 0.5, respectively, vs $k_F R$, and the analytical asymptotics for its average $\tilde{B}(k_F R\sigma)$ [Eq. (B9)].

Figure 10 shows the same averaged quantity $B_\Gamma(u_F\sigma)$ from Eq. (B8) at several values of averaging parameters Γ and ν for which one finds good plateau condition from Fig. 9 versus the variable σ at characteristic values of the two large enough $k_F R$, as examples. The plateau condition (see Figs. 9 and 10) is better with smaller σ and larger semiclassical parameter

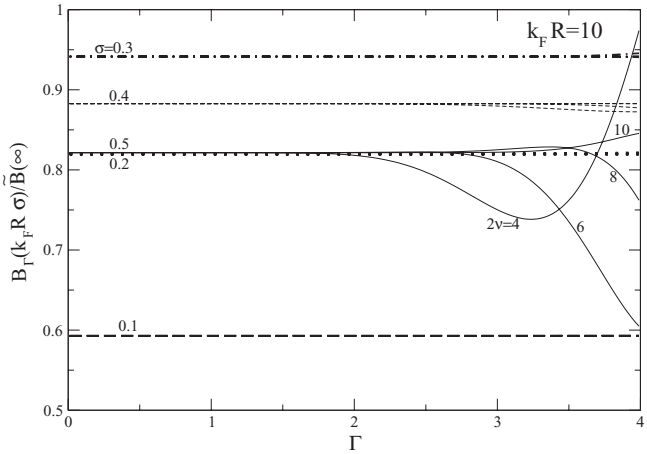

FIG. 9. Study of the plateau condition for the SCM averaged function $B_\Gamma(k_F R\sigma)$ [Eq. (B8)] in the same units of $\tilde{B}(\infty)$ as in Fig. 8 for some characteristic values of σ (numbers on left) vs averaging parameter Γ for several degrees of correction polynomials 2ν (on right); $k_F R = 10$.

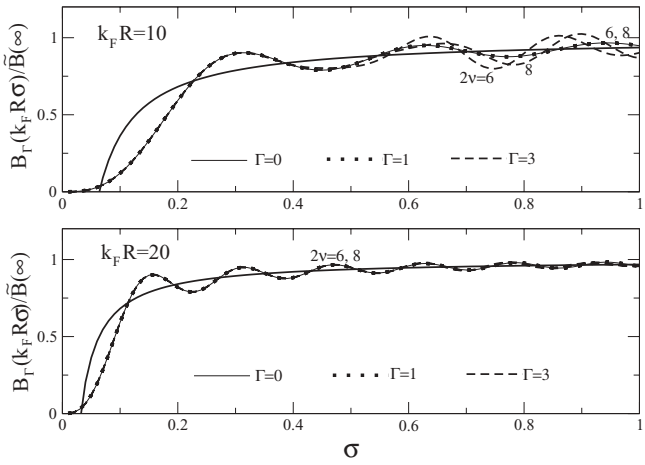

FIG. 10. Averaged function $B_\Gamma(k_F R\sigma)$ [Eq. (B8)] in the same units as in Figs. 8 and 9 vs σ at several characteristic averaging parameters $\Gamma = 0, 1, 3$ and $\nu = 6, 8$ found from the plateau condition in Fig. 9 at two values of $k_F R = 10$ and 20; thick solid lines are its analytical asymptotics from Eq. (B9). The dotted line for $\Gamma = 1$ at all ν and σ coincides with the nonaveraged ($\Gamma = 0$, thin solid) $B(k_F R\sigma)$ [Eq. (B6)] of Fig. 8 within the precision of lines.

$k_F R$. As shown in Fig. 10, the function $B(u_F\sigma)$ has a sharp minimum at zero value of σ with the width of the order of a few relative wave lengths, $1/k_F R$, with respect to the asymptotics for a large argument of $B(u_F\sigma)$. Therefore, the integrals (B4) and (B5) containing $\Delta_B = B - \tilde{B}$ converge in small interval $\sigma \lesssim (1\text{–}3)/k_F R$.

The asymptotics of $\tilde{B}(u_F\sigma)$ in Eq. (B9) at its large argument can be found analytically from Eq. (B8), because the averaging of a polynomial expression in u_F is the same polynomial one if we choose 2ν larger than or equal to the degree of the original polynomial [9,10,12]. In this way, from Eqs. (B8) and (B6), we end at a smooth quantity

$$\tilde{B}(u_F\sigma) = \mathcal{I}\left(\frac{\pi}{4} - \frac{1}{2u_F\sigma}\right), \tag{B9}$$

shown in Fig. 8 by the thick frequent dashed and solid curves at $\sigma = 0.1$ and 0.5, respectively (see also thick solid curves in Fig. 10). On other hand, expanding the function $B(u_F\sigma)$ from Eq. (B6) [shown in Figs. 8 and 10 ($\Gamma = 0$)] in the small semiclassical parameter $1/u_F = 1/k_F R$, one performs then the SCM energy spectrum averaging [9–12,24]. This averaging in $k_F R$ removes oscillating terms proportional to sines and cosines, see Eq. (B6) and Figs. 8–10. Thus, finally, for large enough $k_F R$ from Eqs. (B6) and (B8), one finds a smooth asymptotics $\tilde{B}(u_F\sigma)$ [Eq. (B9)]. As seen from Figs. 8 and 10, this analytical asymptotics (B9) of the averaged quantity $\tilde{B}$ is in good agreement with the numerical average $B_\Gamma(u_F\sigma)$ of Eq. (B8) near the plateau values of the averaging parameters Γ and ν for large enough $k_F R$.

According to Eqs. (B4), (B5), and (B9), the SCM average of the correlationlike terms $\tilde{M}^{(2)}_{QQ}(0)$ [Eq. (B4)] and $\tilde{M}^{(3)}_{QQ}(0)$ [Eq. (B5)] are zeros, because these quantities are linear in Δ_B; i.e., by definition, $\tilde{\Delta}_B = 0$. The part of $\tilde{M}^{(1)}_{QQ}(0)$ [Eq. (B3)] related to the constant $\pi/4$ in $\tilde{B}(u_F\sigma)$ [Eq. (B9)] can be neglected as expressed through the linear correlation function $\langle\hat{Q}(\mathbf{r}+\mathbf{s}/2)\hat{Q}(\mathbf{r}-\mathbf{s}/2) - \hat{Q}^2(\mathbf{r})\rangle_{\rm av}$ averaged in phase-space variables [8,28,35,36], as explained in Sec. III.

Integrating now analytically the remaining integrals over σ and $\wp$ in both Eq. (B1) for $\tilde{M}^{(0)}_{QQ}(0)$ and the nonzero component of Eq. (B3) for $\tilde{M}^{(1)}_{QQ}(0)$, corresponding to the second term in asymptotics (B9) of $\tilde{B}$, with the help of Eqs. (B9) and (B7), one arrives at

$$\tilde{M}^{(0)}_{QQ}(0) \approx \tilde{M}^{(\rm vol)}_{QQ}(0) + \tilde{M}^{(\rm S1)}_{QQ}(0), \quad \tilde{M}^{(1)}_{QQ}(0) \approx \tilde{M}^{(\rm S2)}_{QQ}(0), \tag{B10}$$

where $\tilde{M}^{(\rm vol)}_{QQ}(0)$ is the local-volume inertia part [Eq. (27)]. The latter is related to the first constant term of the macroscopic ($k_F R \to \infty$) asymptotics (B9) in Eq. (B1) [the upper index "vol" is omitted in the left-hand side of Eq. (27)]. For the two surface corrections in Eq. (B10), one obtains

$$\tilde{M}^{(S1)}_{QQ}(0) = \frac{\mathcal{I}\,\zeta^{(1)}_L}{12\,u_F}, \quad \tilde{M}^{(S2)}_{QQ}(0) = \frac{\mathcal{I}\,\zeta^{(2)}_L}{12\,u_F}, \tag{B11}$$

where $\zeta^{(1)}_L$ and $\zeta^{(2)}_L$ are number constants given immediately after Eq. (39).

Collecting all the volume (local) [Eq. (27)], surface [$\sim 1/k_F R$, see Eq. (B11) of Eq. (B10)], and curvature [$\sim 1/(k_F R)^2$] corrections from Eq. (A8) for κ_{FF} and Eq. (A10) for κ_{QQ}, as well as originated by means of Eq. (33) as consistency corrections [$\propto \gamma^2_{QQ}(0)$] in Eq. (10), one finally arrives at the complete ETF inertia M_{FF} [Eq. (39)].

APPENDIX C: FRICTION

Using the approximation (24) for G_0 in the friction $\tilde{\gamma}_{QQ}(0)$ of Eq. (26) and the same coordinate systems as in the derivations of the inertia $\tilde{M}_{QQ}(0)$, in the nearly local case (i), one obtains

$$\tilde{\gamma}_{QQ}(0) = \tilde{\gamma}^{(0)}_{QQ}(0) + \tilde{\gamma}^{(1)}_{QQ}(0) + \tilde{\gamma}^{(2)}_{QQ}(0), \tag{C1}$$

where $\tilde{\gamma}^{(0)}_{QQ}(0)$ is the volume local part [Eq. (28)],

$$\tilde{\gamma}^{(1)}_{QQ}(0) = \frac{\mathcal{I}\hbar}{mR^2}\left\langle \int_0^1 d\wp\, \wp^{2(L+1)} \times \int_0^{1+\wp} d\sigma \left[\sin^2(u_F\sigma) - \frac{1}{2}\right]\right\rangle_{\rm av}, \tag{C2}$$

$$\tilde{\gamma}^{(2)}_{QQ}(0) = \frac{\mathcal{I}\hbar}{mR^2}\left\langle \int_0^1 d\wp\, \wp^{2(L+1)} \int_0^{1+\wp} d\sigma\, \Delta_Q(\sigma/\wp) \times \left[\sin^2(u_F\sigma) - \frac{1}{2}\right]\right\rangle_{\rm av}. \tag{C3}$$

We neglected the linear correlation function $\langle\hat{Q}(\mathbf{r}+\mathbf{s}/2)\hat{Q}(\mathbf{r}-\mathbf{s}/2) - \hat{Q}^2(\mathbf{r})\rangle_{\rm av}$, averaged in phase-space variables, as in the derivations of the inertia [8,35,36].

The phase-space averaging in Eqs. (C2) and (C3) can be exchanged with the integrations over the spatial coordinates. As far as $\langle\sin^2(u_F\sigma) - \frac{1}{2}\rangle_{\rm av} = 0$, the corrections (C2) for $\tilde{\gamma}^{(1)}_{QQ}(0)$ and (C3) for $\tilde{\gamma}^{(2)}_{QQ}(0)$ are zeros. Therefore, we are left with the single local term within the approximation (i).

APPENDIX D: ISOLATED SUSCEPTIBILITY

As in the case of inertia and friction derivations, for the averaged isolated susceptibility

$$\tilde{\chi}_{QQ}(0) = \frac{2d_s}{\pi}\left\langle \int \mathrm{d}\mathbf{r} \int \mathrm{d}\mathbf{s}\ \hat{Q}\left(\mathbf{r}+\frac{\mathbf{s}}{2}\right)\hat{Q}\left(\mathbf{r}-\frac{\mathbf{s}}{2}\right) \times \int_0^\infty \mathrm{d}\varepsilon\, n(\varepsilon)\mathrm{Im}\, G_0\left(\mathbf{r}+\frac{\mathbf{s}}{2},\mathbf{r}-\frac{\mathbf{s}}{2},\varepsilon\right) \times \mathrm{Re}\, G_0\left(\mathbf{r}+\frac{\mathbf{s}}{2},\mathbf{r}-\frac{\mathbf{s}}{2},\varepsilon\right)\right\rangle_{\mathrm{av}}, \quad \text{(D1)}$$

one finds

$$\tilde{\chi}_{QQ}(0) = \tilde{\chi}^{(0)}_{QQ}(0) + \tilde{\chi}^{(1)}_{QQ}(0) + \tilde{\chi}^{(2)}_{QQ}(0), \quad \text{(D2)}$$

where $\tilde{\chi}^{(0)}_{QQ}(0)$ is the volume local part [Eq. (29)],

$$\tilde{\chi}^{(1)}_{QQ}(0) = -\frac{\mathcal{I}\, y_F\, \hbar^2}{2\, m^2\, R^4} \times \left\langle \int_0^1 d\wp\ \wp^{2(L+1)}\ j_0(u_F(1+\wp))\right\rangle_{\mathrm{av}}, \quad \text{(D3)}$$

$$\tilde{\chi}^{(2)}_{QQ}(0) = \frac{\mathcal{I}\, y_F^2\, \hbar^2}{m^2\, R^4}\left\langle \int_0^1 d\wp\ \wp^{2(L+1)} \times \int_0^{1+\wp} d\sigma\ \Delta_Q(\sigma/\wp) j_1(u_F\sigma)\right\rangle_{\mathrm{av}}. \quad \text{(D4)}$$

We removed again the zero linear correlation function $\langle \hat{Q}(\mathbf{r}+\mathbf{s}/2)\hat{Q}(\mathbf{r}-\mathbf{s}/2) - \hat{Q}^2(\mathbf{r})\rangle_{\mathrm{av}}$, averaged in phase-space variables. Note that the splitting into the two terms, the local $\tilde{\chi}^{(0)}_{QQ}(0)$ [Eq. (29)] and its correction $\tilde{\chi}^{(1)}_{QQ}(0)$, was found after the integration of $j_1(w)$ over its argument $w = 2u_F\sigma$, in Eq. (D1), as integrand values at lower and upper limits of the integral over w.

The phase-space averaging in Eqs. (D3) and (D4) can be again exchanged with the integration over the spatial coordinate $\wp$. Therefore, the leading term of the average $\langle j_1(u_F\sigma)\rangle_{\mathrm{av}}$ at large $k_F R$ is vanishing due to its SCM part and the corrections (D3) for $\tilde{\chi}^{(1)}_{QQ}(0)$ and (D4) for $\tilde{\chi}^{(2)}_{QQ}(0)$ are approximately zero. Thus, within approach (i), we are left with the only local term $\chi^{(0)}_{QQ}(0)$ of Eq. (29).

[1] A. Bohr and B. Mottelson, *Nuclear Structure* (Benjamin, New York, 1975), Vol. II.
[2] A. B. Migdal, *The Finite Fermi-System Theory and Atomic Nuclear Properties* (Nauka, Moscow, 1983) (in Russian).
[3] G. F. Bertsch, P. F. Bortignon, and R. A. Broglia, Rev. Mod. Phys. **55**, 287 (1983).
[4] H. Hofmann, Phys. Rep. **284**, 137 (1997).
[5] R. A. Broglia, R. Barrancho, G. F. Bertsch, and E. Vigezzi, Phys. Rev. C **49**, 552 (1994).
[6] V. I. Abrosimov, A. Dellafiore, and F. Matera, Nucl. Phys. **A653**, 115 (1999); **A717**, 44 (2003).
[7] V. I. Abrosimov, D. M. Brink, A. Dellafiore, and F. Matera, arXiv:nucl-th/0407015.
[8] V. M. Strutinsky, A. G. Magner, and M. Brack, Z. Phys. A **316**, 217 (1984).
[9] A. G. Magner, A. M. Gzhebinsky, and S. N. Fedotkin, Phys. Atom. Nucl. **70**, 1859 (2007).
[10] V. M. Strutinsky, Nucl. Phys. **A95**, 420 (1967); **A122**, 1 (1968).
[11] M. Brack, L. Damgard, A. S. Jensen *et al.*, Rev. Mod. Phys. **44**, 320 (1972).
[12] M. Brack and R. K. Bhaduri, *Semiclassical Physics, Frontiers in Physics*, Vol. 96, second edition (Westview Press, Boulder CO, USA, 2003).
[13] M. Gutzwiller, *Chaos in Classical and Quantum Mechanics* (Springer-Verlag, New York, 1990).
[14] R. B. Balian and C. Bloch, Ann. Phys. (NY) **69**, 76 (1972).
[15] V. M. Strutinsky and A. G. Magner, Sov. Phys. Part. Nucl. **7**, 138 (1976).
[16] A. G. Magner, K. Arita, S. N. Fedotkin, and K. Matsuyanagi, Prog. Theor. Phys. **108**, 853 (2002).
[17] A. G. Magner, S. M. Vydrug-Vlasenko, and H. Hofmann, Nucl. Phys. **A524**, 31 (1991).
[18] J. Blocki, Y. Bonch, J. R. Nix, and W. J. Swiatecki, Ann. Phys. (NY) **113**, 330 (1978).
[19] S. E. Koonin, R. L. Hatch, and J. Randrup, Nucl. Phys. **A283**, 87 (1977).
[20] S. E. Koonin and J. Randrup, Nucl. Phys. **A289**, 475 (1977).
[21] C. Yannouleas and R. A. Broglia, Ann. Phys. (NY) **217**, 105 (1992).
[22] H. Hofmann, F. A. Ivanyuk, and S. Yamaji, Nucl. Phys. **A598**, 187 (1996).
[23] F. A. Ivanyuk, H. Hofmann, V. V. Pashkevich, and S. Yamaji, Phys. Rev. C **55**, 1730 (1997).
[24] A. G. Magner, A. M. Gzhebinsky, and S. N. Fedotkin, Phys. Atom. Nucl. **70**, 647 (2007).
[25] V. M. Strutinsky, A. G. Magner, and M. Brack, Z. Phys. A **318**, 205 (1984).
[26] V. M. Strutinsky, A. G. Magner, and V. Yu. Denisov, Z. Phys. A **322**, 149 (1985).
[27] A. G. Magner and V. M. Strutinsky, Z. Phys. A **322**, 633 (1985).
[28] V. M. Kolomietz, A. G. Magner, and V. A. Plujko, Sov. J. Nucl. Phys. **55**, 1143 (1992); Z. Phys. A **345**, 131 (1993).
[29] A. G. Magner, V. M. Kolomietz, H. Hofmann, and S. Shlomo, Phys. Rev. C **51**, 2457 (1995).
[30] V. M. Kolomietz, A. G. Magner, and S. Shlomo, Phys. Rev. C **73**, 024312 (2006).
[31] S. Raman, Jr., C. W. Nestor, and P. Tikkanen, At. Data Nucl. Data Tables **78**, 1 (2001).
[32] T. Kibedi and R. H. Spear, At. Data Nucl. Data Tables **89**, 77 (2005).
[33] T. Belgya, O. Bersillon, R. Capote, T. Fukahori, G. Zhigang, S. Goriely, M. Herman, A. V. Ignatyuk, S. Kailas, A. Koning, P. Oblozinsky, V. Plujko, and P. Young, *IAEA-TECDOC-1506: Handbook for Calculations of Nuclear Reaction Data: Reference Input Parameter Library-2* (IAEA, Vienna, 2005), Ch. 7; http://www-nds.iaea.org/RIPL-2/.
[34] H. Hofmann, Phys. Lett. **B61**, 423 (1976).
[35] R. Balescu, *Equilibrium and Non-equilibrium Statistical Mechanics* (Wiley, New York, 1975), Vol. II.
[36] L. P. Kadanoff and G. Baym, *Quantum Statistical Mechanics: Green's Function Method in Equilibrium and Non-equilibrium Problems* (Benjamin, New York, 1962) [Russ. transl. Mir, Moscow, 1964].

[37] V. M. Kolomietz and V. N. Kondratjev, Z. Phys. A **344**, 125 (1992).
[38] A. Bohr and B. Mottelson, *Nuclear Structure* (Benjamin, New York, 1971), Vol. I.
[39] A. G. Magner and V. A. Plujko, Sov. J. Nucl. Phys. **51**, 53 (1990); Izv. Acad. Sci. USSR. Sect. Phys. **54**, 877 (1990).
[40] V. A. Plujko and O. M. Gorbachenko, Sci. Papers Inst. Nucl. Res. **2**, 17 (2005); Phys. At. Nucl. **70**, 1167 (2007).
[41] V. A. Plujko, O. M. Gorbachenko, and I. M. Kadenko, Int. J. Mod. Phys. E **16**, 372 (2007).
[42] A. M. Gzhebinsky, A. G. Magner, and A. S. Sitdikov, Nucl. Phys. At. Energy. **1**, 17 (2007).